

Development of an mRNA-lipid nanoparticle vaccine against Lyme disease

Matthew Pine,^{1,2} Gunjan Arora,³ Thomas M. Hart,³ Emily Bettini,² Brian T. Gaudette,⁴ Hiromi Muramatsu,² István Tombácz,¹ Taku Kambayashi,⁴ Ying K. Tam,⁵ Dustin Brisson,⁶ David Allman,⁴ Michela Locci,² Drew Weissman,¹ Erol Fikrig,³ and Norbert Pardi²

¹Department of Medicine, University of Pennsylvania, Philadelphia, PA 19104, USA; ²Department of Microbiology, Perelman School of Medicine, University of Pennsylvania, Philadelphia, PA 19104, USA; ³Section of Infectious Diseases, Department of Internal Medicine, Yale University School of Medicine, New Haven, CT 06520, USA; ⁴Department of Pathology and Laboratory Medicine, Perelman School of Medicine, University of Pennsylvania, Philadelphia, PA 19104, USA; ⁵Acuitas Therapeutics, Vancouver, BC, Canada; ⁶Department of Biology, University of Pennsylvania, Philadelphia, PA 19104, USA

Lyme disease is the most common vector-borne infectious disease in the United States, in part because a vaccine against it is not currently available for humans. We propose utilizing the lipid nanoparticle-encapsulated nucleoside-modified mRNA (mRNA-LNP) platform to generate a Lyme disease vaccine like the successful clinical vaccines against SARS-CoV-2. Of the antigens expressed by *Borrelia burgdorferi*, the causative agent of Lyme disease, outer surface protein A (OspA) is the most promising candidate for vaccine development. We have designed and synthesized an OspA-encoding mRNA-LNP vaccine and compared its immunogenicity and protective efficacy to an alum-adjuvanted OspA protein subunit vaccine. OspA mRNA-LNP induced superior humoral and cell-mediated immune responses in mice after a single immunization. These potent immune responses resulted in protection against bacterial infection. Our study demonstrates that highly efficient mRNA vaccines can be developed against bacterial targets.

INTRODUCTION

Lyme disease, caused by various species and strains of the bacteria *Borrelia burgdorferi sensu lato*, is the most common vector-borne illness in the United States. Its prevalence and geographic distribution have increased significantly since it was labeled a nationally notifiable condition in 1991.^{1,2} The Centers for Disease Control and Prevention report an estimated 476,000 cases of Lyme disease in the United States annually.³ Early infection manifests itself in a skin rash known as erythema migrans.⁴ Influenza-like symptoms often follow, but symptoms respond rapidly to antibiotics. Lyme disease can be difficult to diagnose, which may lead to delayed treatment and subsequently more severe complications.^{5,6} Carditis, arthritis, and neurological issues are characteristic of late stages of infection.⁷ Lyme disease can impact patients for the remainder of their lives, and, to make matters worse, contracting one strain does not equate with immunity against heterologous strains.⁸ Thus, developing a broadly protective prophylactic vaccine is crucial to preventing new and repeated cases of Lyme disease.

Lyme disease is transmitted through the bite of an *Ixodes* tick carrying the spirochete *Borrelia burgdorferi*. Infection begins with tick saliva

contaminating the site of the bite; it spreads by activating host proteases that digest extracellular matrix components and employing mechanisms to evade immune response in the affected individual.^{9–14}

B. burgdorferi expresses numerous proteins that are potential targets for vaccination. One such antigen is outer surface protein A (OspA), an abundantly expressed surface lipoprotein that anchors the bacterium to the tick midgut. It is rapidly downregulated upon feeding; therefore, early targeting is essential.^{15,16} There are many diverse strains of *B. burgdorferi* in the United States known to infect humans.¹⁷ OspA is a desirable vaccine target compared to other antigens because it is widely conserved among these strains.¹⁸ In 1998, GlaxoSmithKline (GSK) released phase III clinical trial results for LYMERix, an alum-adjuvanted recombinant OspA protein vaccine.¹⁹ Within a year, rates of Lyme disease had decreased by 76% among individuals who were vaccinated. However, a seminal paper was published the same year LYMERix was put on the market that revealed that OspA contained an epitope that was homologous to a peptide in hLFA-1, postulating that this cross-reactivity could lead to the development of treatment-resistant Lyme arthritis.²⁰ Although OspA vaccination was later proven to not cause this autoimmune response, LYMERix was removed from the market in 2002, just 4 years after its release.^{21,22} Since then, baited OspA-based vaccines have been developed that successfully block transmission of *B. burgdorferi* to ticks from their reservoir hosts, mainly *Peromyscus leucopus* (the white-footed mouse).²³ Additionally, OspA-containing Lyme disease vaccines are commercially available for the immunization of dogs.^{24,25} Finally, the most promising candidate for a human Lyme disease vaccine (VLA15), which has begun phase III efficacy studies (NCT05477524), is OspA-based.²⁶

There has been no FDA-approved vaccine for Lyme disease since the demise of LYMERix, and cases continue to rise, underscoring the need

Received 2 February 2023; accepted 28 July 2023;
<https://doi.org/10.1016/j.ymthe.2023.07.022>

Correspondence: Norbert Pardi, Department of Microbiology, Perelman School of Medicine, University of Pennsylvania, Philadelphia, PA 19104, USA.

E-mail: pnorbert@pennmedicine.upenn.edu

for a preventative approach. An ideal vaccine is safe and efficacious, inducing broad protection in a variety of immunological backgrounds. Many preclinical Lyme disease vaccine candidates are inadequate as they elicit only strain-specific immunity after administration of multiple vaccine doses.²⁷

Lipid nanoparticle (LNP)-encapsulated nucleoside-modified mRNA-based vaccines demonstrated their safety and potency against various infectious diseases in preclinical studies^{28–33} as well as in human trials, and significantly contributed to the mitigation of the devastating effects of the coronavirus disease 2019 (COVID-19) pandemic.^{34–36} The mRNA-LNP vaccine platform induced potent antibody and cellular immune responses in both animals and humans, highlighting the viability of this novel modality for vaccine delivery. Here, we demonstrate that, in mice, OspA-encoding nucleoside-modified mRNA-LNP displays superior immunogenicity to an alum-adjuvanted OspA protein subunit vaccine at doses of 3 µg and 1 µg, respectively. The robust, antigen-specific humoral and cellular responses corresponded to protection against the heterologous N40 strain of *B. burgdorferi*. Applying nucleoside-modified OspA mRNA-LNP to *B. burgdorferi* could potentially reduce the prevalence of Lyme disease in the United States.

RESULTS

OspA mRNA-LNP vaccination yields robust innate immune cell infiltration and antigen-specific CD4⁺ and CD8⁺ T cell responses in mice

Prior to the immunization studies, protein production from the OspA mRNA was demonstrated *in vitro* (Figure S1). Neuro 2-a cells were transfected with OspA- and firefly luciferase (Luc, negative control)-encoding mRNAs, and OspA protein in cell lysates was detected by western blotting.

Next, Balb/c mice were immunized intramuscularly with a single dose of 3 µg mRNA-LNP encoding OspA or 1 µg alum-adjuvanted OspA protein (rOspA + alum, positive control). Frequencies of innate cells (neutrophils, dendritic cells [DCs], macrophages, and monocytes) at the site of injection were measured at days 1, 3, and 5 post immunization. Non-injected animals (day 0) were used as controls. In both vaccine groups, infiltration of neutrophils peaked at day 1 and DCs, macrophages, and monocytes at day 3, and all populations decreased by day 5 (Figures S2 and S3).

In a separate study, Balb/c mice were immunized intramuscularly with a single dose of 3 µg OspA or Luc mRNA-LNP or 1 µg rOspA + alum. OspA-specific CD4⁺ and CD8⁺ T cell responses were evaluated after 12 days by intracellular cytokine staining of splenocytes (Figure 1A). The OspA mRNA-LNP vaccine elicited significantly higher levels of antigen-specific CD4⁺ and CD8⁺ T cells expressing Th1-associated cytokines (interferon [IFN]-γ, interleukin [IL]-2, and tumor necrosis factor [TNF]-α) than either Luc mRNA-LNP or rOspA + alum (Figures S4, 1B, and 1C). The only subpopulation that was not significantly increased compared to other experimental groups was IL-2⁺ CD8⁺ T cells, which are not major producers of

this cytokine.³⁷ Both CD4⁺ and CD8⁺ T cell responses to immunization with OspA mRNA-LNP were polyfunctional (Figures 1D and 1E). Hence, these data show that a single dose of OspA mRNA-LNP produced antigen-specific cellular immune responses in the spleens of mice.

OspA mRNA-LNP vaccination elicits robust levels of Tfh cells and antigen-specific GC B cells in mice

Immunization with nucleoside-modified mRNA-LNP vaccines has previously shown to induce high levels of antigen-specific CD4⁺ T cells, especially T follicular helper (Tfh) cells, as well as germinal center B (GC B) cells, which work together in the germinal centers to ultimately generate high-affinity antibodies.^{38–41} To evaluate Tfh cell and GC B cell responses after OspA mRNA-LNP vaccination, Balb/c mice were immunized with the same dosing and treatment regimens as described above and sacrificed after 12 days as in the previous study. Popliteal and inguinal draining lymph nodes (dLNs) as well as spleens were harvested, and Tfh cells and antigen-specific GC B cells were analyzed by flow cytometry. In the dLNs of animals immunized with OspA mRNA-LNP, there was a significantly higher frequency and total number of CXCR5⁺PD-1⁺ Tfh cells compared to those in mice vaccinated with either Luc mRNA-LNP or rOspA + alum (Figures 2A and 2B). There were no statistically significant differences in Tfh cell responses in the spleens (Figure S5A). Furthermore, as Tfh cells provide help in the germinal center reaction, we hypothesized that there would be robust levels of GC B cells in OspA mRNA-LNP-immunized animals. To test this hypothesis, we generated fluorescently labeled tetrameric OspA probes to identify OspA-specific B cells, as previously described for other antigens.^{39,41,42} As anticipated, the dLNs of animals immunized with OspA mRNA-LNP exhibited significantly higher frequency and total number of OspA-specific FAS⁺GL7⁺ GC B cells than in those administered either with Luc mRNA-LNP or rOspA + alum (Figures 2C and 2D). There were no statistically significant differences in GC B cell responses in the spleens (Figure S5B). Collectively, these data show that a single immunization of OspA mRNA-LNP generates robust germinal center response in the draining lymph nodes of mice.

OspA mRNA-LNP vaccination induces potent antigen-specific memory B cell and long-lived plasma cell responses in mice

Balb/c mice were immunized with the same dosing and treatment regimen as in the previous studies described above. Animals were sacrificed 8 weeks post vaccination, and spleens and bone marrow were collected to assess immunological memory by flow cytometry. The germinal center response gives rise to memory B cells (MBCs), which can be activated when called upon by potential infection, and long-lived plasma cells (LLPCs), which secrete high-affinity antibodies.⁴³ In the spleens of immunized mice, the total number of antigen-specific CD38⁺GL7[−] MBCs was significantly higher than in naive animals as well as those vaccinated with either Luc mRNA-LNP or rOspA + alum (Figures 3A and 3B). Furthermore, frequency of antigen-specific B220[−]CD138⁺ LLPCs in the bone marrow of mice immunized with OspA mRNA-LNP was significantly increased compared to those vaccinated with Luc mRNA-LNP. In contrast,

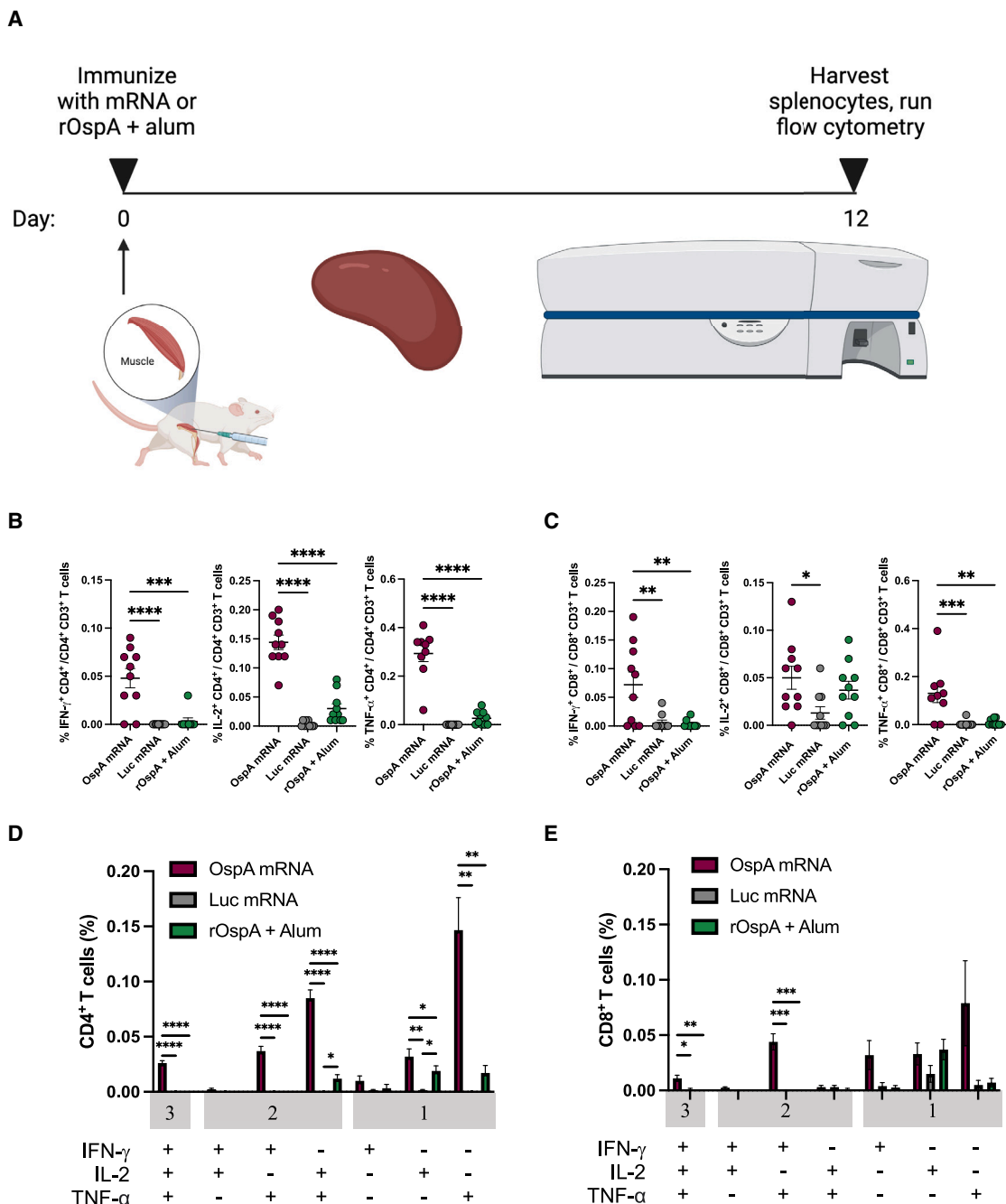


Figure 1. Nucleoside-modified OspA mRNA-LNP vaccination induces antigen-specific T cell responses in mice

(A) Mice were vaccinated intramuscularly with a single dose of 3 μ g of OspA mRNA-LNP or 3 μ g of Luc mRNA-LNP or 1 μ g of rOspA + alum. Splenocytes were stimulated with an OspA overlapping peptide pool 12 days after immunization, and cytokine production by CD4⁺ and CD8⁺ T cells was analyzed by flow cytometry. Percentages of OspA-specific (B) CD4⁺ and (C) CD8⁺ T cells producing IFN- γ , IL-2, and TNF- α and frequencies of combinations of cytokines produced by (D) CD4⁺ and (E) CD8⁺ T cells are shown. Values from OspA-immunized mice are compared to values from animals immunized with Luc mRNA-LNP or rOspA + alum (B, C, D, and E). Each symbol represents one animal, and data represent mean \pm SEM (n = 9–10 mice per group). Data from two independent experiments are shown. Statistical analysis: one-way ANOVA with Bonferroni correction, *p < 0.05, **p < 0.01, ***p < 0.001, ****p < 0.0001.

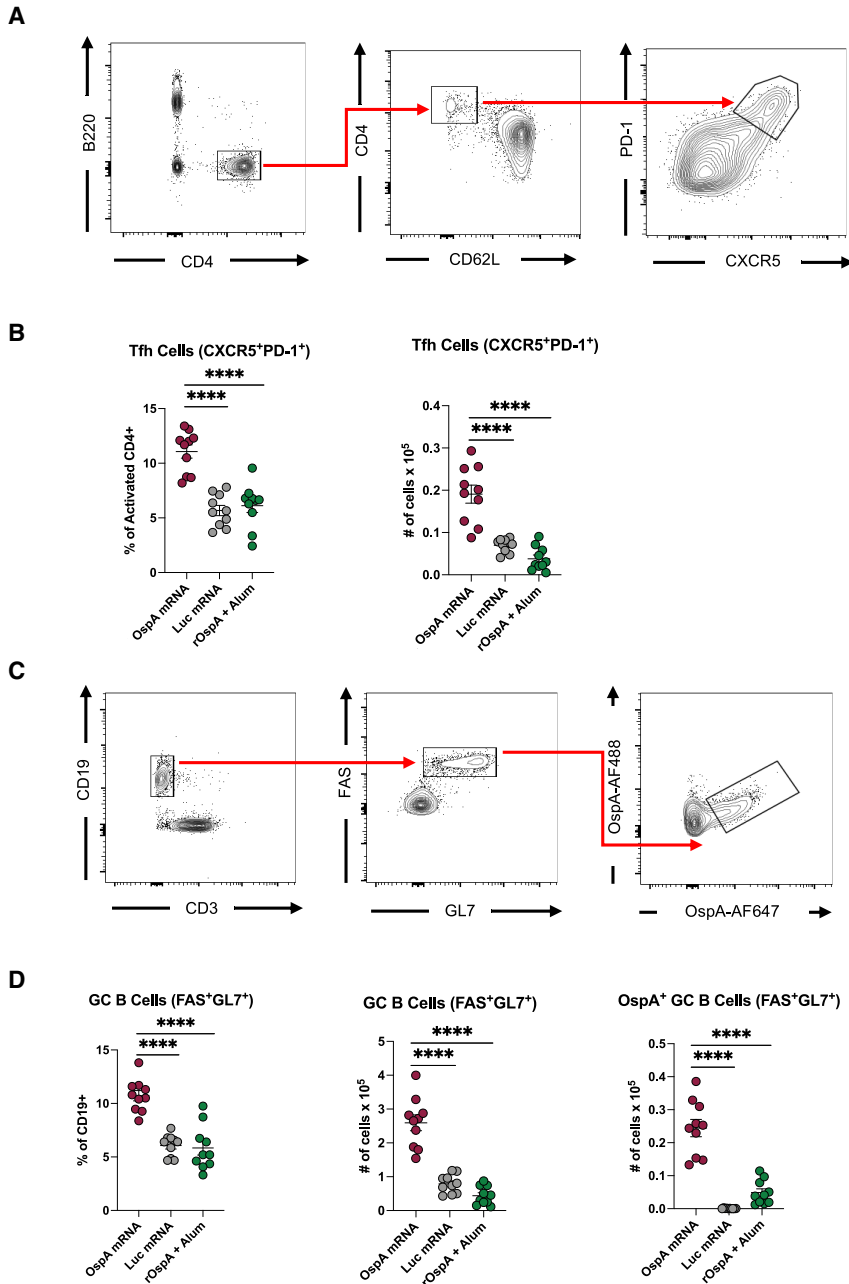


Figure 2. Nucleoside-modified OspA mRNA-LNP yields Tfh cell and antigen-specific GC B cell responses in mice

Mice were vaccinated intramuscularly with OspA or Luc mRNA-LNP or rOspA + alum as described in Figure 1. Tfh and GC B cell responses in inguinal and popliteal lymph nodes were analyzed at day 12 post immunization. (A and B) Tfh cell (B220⁻CD4⁺CD62L⁻PD-1⁺CXCR5⁺) representative gating strategy (A) and frequencies and absolute numbers (B). (C and D) Antigen-specific GC B cell (CD19⁺CD3⁻FAS⁺GL7⁺OspA-AF488⁺/OspA-AF647⁺) representative gating strategy (C) and frequencies and absolute numbers, including non-specific GC B cells (D). Each symbol represents one animal, and data represent mean ± SEM (n = 10 mice per group). Data from two independent experiments are shown. Statistical analysis: one-way ANOVA with Bonferroni correction, *p < 0.05, **p < 0.01, ***p < 0.001, ****p < 0.0001.

Prime and boost with the OspA mRNA-LNP vaccine generates durable antibody response in mice

Balb/c mice were immunized intramuscularly with 3 µg mRNA-LNP encoding either OspA or Luc or 1 µg rOspA + alum. Animals were bled 2 weeks post vaccination, and serum was collected. At 4 weeks post immunization, mice were bled again, and each group received a booster of the same treatment that was equivalent to the prime dose. Animals were bled again at 8, 16, and 24 weeks after the initial injection, and serum was obtained (Figure 4A). To test for the presence of OspA-specific antibodies in the sera, binding to recombinant OspA protein was assessed by enzyme-linked immunosorbent assay (ELISA). 2 and 4 weeks after the prime dose, OspA-specific IgG titers were significantly higher in the OspA mRNA-LNP-immunized group than in the Luc mRNA-LNP or rOspA + alum groups. 4 weeks after administration of respective booster doses (week 8), OspA-specific IgG titers were also significantly increased in the OspA mRNA group compared to the Luc mRNA and alum-adju- vanted rOspA groups, a result that held up to

the frequency of this LLPC population in animals administered rOspA + alum was not significantly greater than in the negative control group (Figures 3C and 3D). Additionally, levels of various IgG subtypes in the bone marrow were measured by ELISpot. Mice immunized with OspA mRNA-LNP displayed a broad antibody response with detectable levels of IgG1, IgG2a, and IgG2b (Figure 3E), which is consistent with previous findings of SARS-CoV-2 mRNA-LNP vaccine studies.⁴⁴ These data reveal that a single vaccination with OspA mRNA-LNP elicits memory B cell and long-lived plasma cell response in mice.

24 weeks post prime (Figure 4B). These data show that a prime-boost regimen of OspA mRNA-LNP yields durable levels of antigen-specific antibodies in mice that persist for at least 24 weeks after initial immunization.

A single immunization with OspA mRNA-LNP protects mice from challenge with *Borrelia burgdorferi*

Balb/c mice were immunized intramuscularly with a single dose of 3 µg OspA or Luc mRNA-LNP or 1 µg rOspA + alum. 4 weeks after vaccination, animals were challenged via subcutaneous injection with

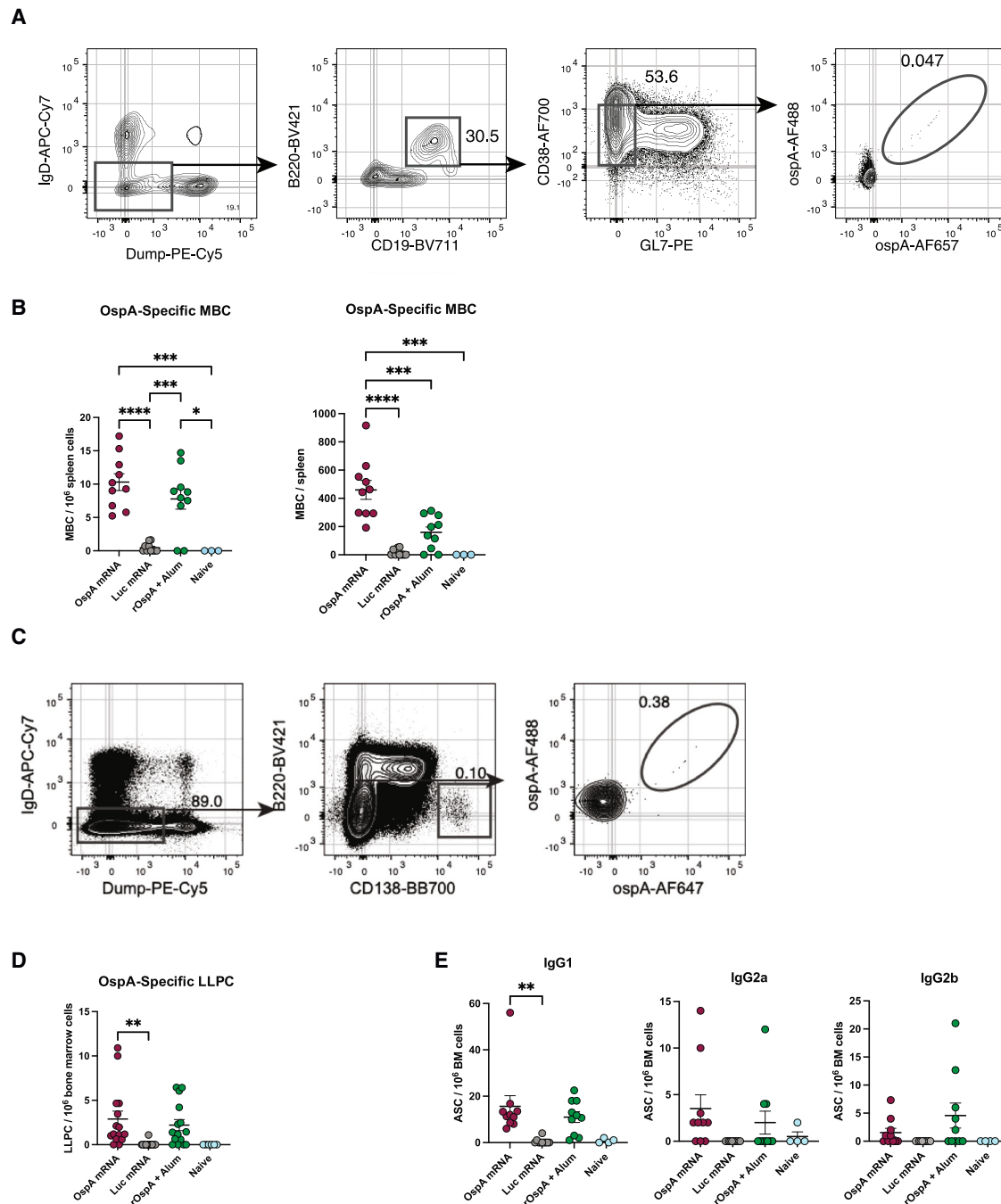
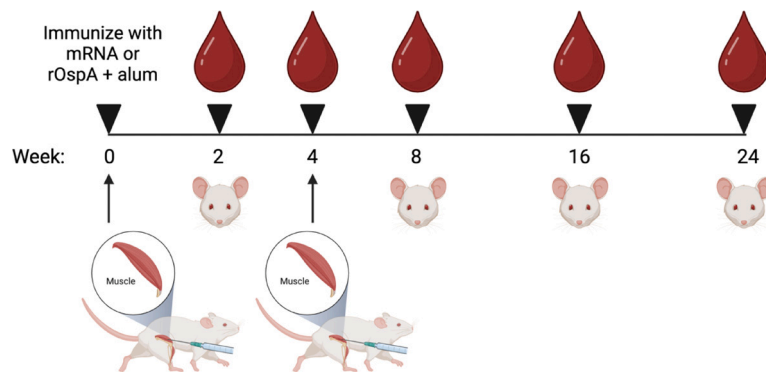


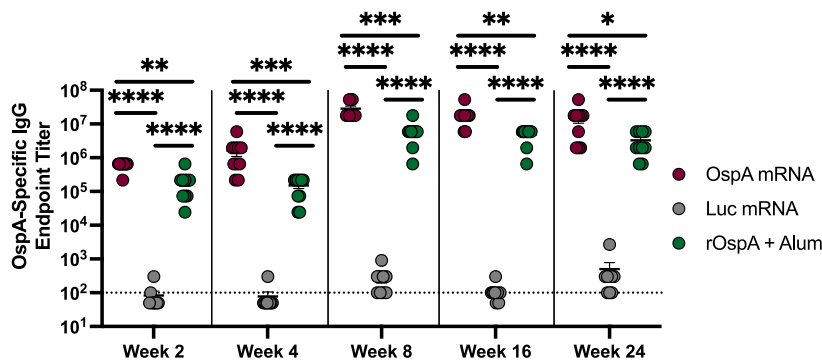
Figure 3. Nucleoside-modified OspA mRNA-LNP vaccination elicits potent antigen-specific MBC and LLPC responses in mice

Mice were vaccinated intramuscularly with OspA or Luc mRNA-LNP or rOspA + alum as described in Figure 1. MBCs and LLPCs in spleen and bone marrow, respectively, were analyzed 8 weeks post immunization. (A and B) Antigen-specific MBC (IgD⁻Dump[CD4, CD8a, Ter-119, F4/80]⁻CD19⁺B220⁺CD38⁺GL7⁻OspA-AF488⁺/OspA-AF647⁺) representative gating strategy (A) frequency and absolute numbers (B). (C and D) Antigen-specific LLPC (IgD⁻Dump[CD4, CD8a, Ter-119, F4/80]⁻B220⁻CD138⁺OspA-AF488⁺/OspA-AF647⁺) representative gating strategy (C) and frequency (D). (E) Quantification of bone marrow OspA-specific IgG1, IgG2a, and IgG2b antigen secreting cells (ASCs). In (B), (D), and (E), each symbol represents one animal, and data represent mean \pm SEM (n = 10–15 mice per group except for naive, in which n = 3–6). Data from two to three independent experiments are shown. Statistical analysis: one-way ANOVA with Bonferroni correction, *p < 0.05, **p < 0.01, ***p < 0.001, ****p < 0.0001.

A



B



1×10^5 low-passage *B. burgdorferi* spirochetes (strain N40). Mice were sacrificed 25 days post-infection, and bladder, heart, joint (knee), and skin (ear) samples were collected (Figure 5A). The same tissues were also gathered from uninfected Balb/c mice to measure background. After DNA extraction, quantitative polymerase chain reaction (qPCR) was performed to test for the presence of *flagellin* (*flaB*), a *Borrelia*-specific gene used to measure *B. burgdorferi* burden in tissues. Levels of *flaB* were normalized by comparison with the mouse β -actin gene.⁴⁵ As expected, Luc mRNA-LNP immunized mice had significantly higher bladder, heart, and ear *Borrelia* burdens when compared to naive mice. This trend was also observable when comparing levels of *flaB* in the knees of these two groups (Figure 5B). Furthermore, *Borrelia* burdens were significantly lower in the bladders, hearts, and ears (skin) of OspA mRNA-LNP-immunized mice (means = 6.25×10^{-6} , 2.63×10^{-5} , 2.61×10^{-7} , respectively) than in mice vaccinated with the negative control Luc mRNA-LNP (means = 3.93×10^{-5} , 6.21×10^{-5} , 7.04×10^{-5} , respectively). *Borrelia* burdens also trended toward being lower in the knees (joint) of OspA mRNA-LNP immunized mice (mean = 3.67×10^{-6}) than in mice vaccinated with Luc mRNA-LNP (mean = 2.37×10^{-5}). Interestingly, mice immunized with rOspA + alum had significantly lower bacterial burdens only in the heart and ears when compared with Luc mRNA-LNP vaccinated mice, while no differences were detected in the bladders and knees. Moreover, bacterial burdens were significantly higher

Figure 4. Nucleoside-modified OspA mRNA-LNP vaccination generates long-term antibody responses in mice

(A) Mice were vaccinated intramuscularly with a single dose of 3 μ g of OspA or Luc mRNA-LNP or 1 μ g of rOspA + alum (represented by upward arrow) and bled retro-orbitally at 2 weeks (represented by blood droplet). Mice were bled again at 4 weeks and boosted with the same vaccine doses and then subsequently bled up to 24 weeks. (B) OspA-specific IgG endpoint titers from OspA mRNA-LNP-immunized mice are compared to values from animals immunized with 3 μ g Luc or 1 μ g rOspA + alum (and boosted with same dose at 4 weeks). Each symbol represents one animal, and data represent mean \pm SEM ($n = 9$ –10 mice per group). The horizontal dotted line represents the limit of detection. Titrations below the limit of detection are reported as half of the limit of detection. Data from two independent experiments are shown. Statistical analysis: one-way ANOVA with Bonferroni correction of log transformed data, * $p < 0.05$, ** $p < 0.01$, *** $p < 0.001$, **** $p < 0.0001$.

in the bladders of rOspA + alum immunized mice than in those vaccinated with OspA mRNA-LNP (Figure 5B). To further test for evidence of *B. burgdorferi* infection, an ELISA against C₆, a peptide derived from the sixth invariant region of the *Borrelia* VlsE lipoprotein, was performed with sera from mice 25 days post infection. Binding to C₆ was significantly higher in Luc mRNA-LNP-immunized mice than in those vaccinated

with OspA mRNA-LNP or rOspA + alum or naive mice, indicating that all mice in the negative control group were infected (Figure 5C). Collectively, mice were considered protected when their *flaB* levels in all tissues analyzed were less than the average plus standard deviation of the *flaB* levels in naive mice (bladder = 2.64×10^{-5} , heart = 3.50×10^{-5} , joint = 1.48×10^{-5} , skin = 4.35×10^{-6}). Taken together, 0 out of 10 Luc mRNA-LNP mice, 5 out of 10 rOspA + alum mice, and 8 out of 10 OspA mRNA-LNP mice were protected. These findings demonstrate that vaccination with OspA mRNA-LNP is highly protective. In a separate study, *B. burgdorferi* was detected by culture in the spleens of all mice vaccinated twice with Luc mRNA-LNP and none of the animals that received two doses of OspA mRNA-LNP or rOspA + alum (Figure S6).

DISCUSSION

Lyme disease is the most common vector-borne disease in the United States, and the prevalence of cases and regions in which it occurs have grown in recent years.⁴⁶ Between 2004 and 2016 alone, the total number of tick-borne disease (TBD) cases in the United States doubled, amounting to 77% of all reported vector-borne disease cases during that time. Lyme disease on its own accounted for 82% of those TBD cases.⁴⁷ Infection with *Borrelia burgdorferi*, which is transmitted through the bite of an *Ixodes* tick, is treatable with antibiotics. However, high incidence of arthritis in Connecticut (USA) in the 1970s

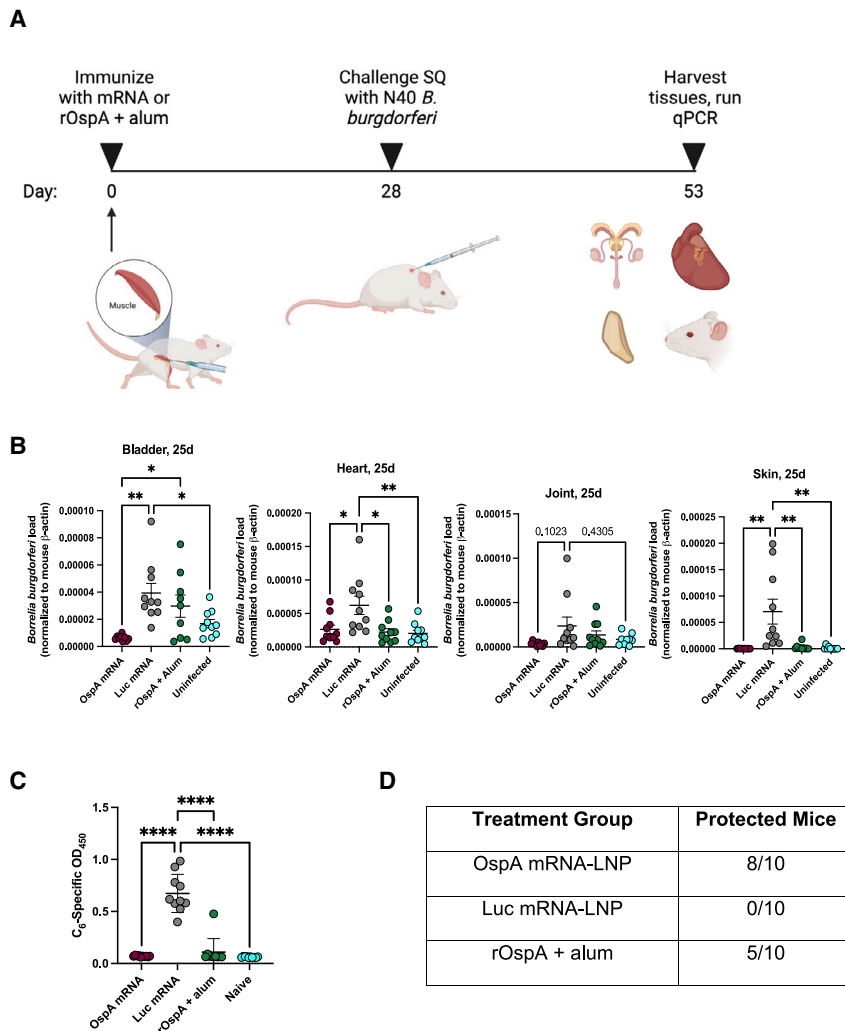


Figure 5. Nucleoside-modified OspA mRNA-LNP vaccination protects mice from infection with *Borrelia burgdorferi*

(A) Mice were vaccinated with a single dose of OspA or Luc mRNA-LNP or rOspA + alum (represented by upward arrow) as described in Figure 1. 28 days after immunization, mice were challenged subcutaneously (SQ) with 10^5 *Borrelia burgdorferi* (strain N40) and then sacrificed 25 days later. Bladder, heart, joint (knee), and skin (ear) tissues were harvested for detection of *B. burgdorferi* infection. (B) qPCR results showing *Borrelia*-specific gene (*flaB*) normalized to mouse β -actin in bladder, heart, joint, and skin. Each symbol represents one animal, and data represent mean \pm SEM ($n = 9$ – 10 mice per group). (C) Binding of sera samples 25 days post-infection to C₆ protein by ELISA. (D) Numbers of protected mice by treatment group. Data from two independent experiments are shown. Statistical analysis: one-way ANOVA with Bonferroni correction, * $p < 0.05$, ** $p < 0.01$, *** $p < 0.001$, **** $p < 0.0001$.

ical trials (NCT04801420) and has begun phase III efficacy studies (NCT05477524), once again highlighting the safety of this antigen.⁵³ VLA15 is a hexavalent formulation of six OspA serotypes from not only *B. burgdorferi* but also other *Borrelia* species that cause Lyme disease in Europe.⁵⁴ Although recombinant protein is a well-established vaccine platform, nucleoside-modified mRNA-LNP vaccines often display more robust immunogenicity and efficacy profiles that warrant exploring their application to Lyme disease.

Nucleoside-modified mRNA-LNPs offer numerous advantages over recombinant protein and other vaccine platforms. Generating and purifying recombinant proteins or growing viruses is

a process that expends time and resources, whereas mRNA synthesis is much more rapid and scalable.^{33,55} Additionally, some mRNA-LNP vaccines have shown superiority over adjuvanted protein subunit and inactivated virus vaccines in comparative preclinical studies.^{29,38,56}

The effectiveness of nucleoside-modified mRNA-LNP has translated to humans as they induce potent antibody and cellular immune responses against SARS-CoV-2, the causative agent of COVID-19.³⁴ Importantly, mRNA vaccines have been developed against many viral targets, but there are few studies that described mRNA vaccines against bacteria or other pathogens.^{57–61} Bacteria and parasites are much more complex than viruses as they often contain numerous antigens with ill-defined protective immune responses.^{62,63} The mRNA-LNP platform has already shown that it is applicable to Lyme disease as immunization with 19ISP, a formulation of 19 different tick salivary proteins, protected guinea pigs from infection with *B. burgdorferi*.⁵⁹ The development of an OspA-based mRNA-LNP vaccine is significant as it is one of the first mRNA vaccines to target a non-viral pathogen.

first demonstrated that chronic late-stage manifestations could arise if Lyme disease were left untreated.⁴⁸ Furthermore, post-treatment Lyme disease syndrome (PTLDS) encompasses long-lasting symptoms such as severe joint pain and neurocognitive issues that patients experience even after a course of oral (usually doxycycline) or intravenous (usually ceftriaxone) antibiotics.^{49,50}

The pervasiveness of Lyme disease and severity of PTLDS symptoms underscores the need for a prophylactic vaccine to protect individuals from infection with *B. burgdorferi*. Despite the strong safety and efficacy profiles that LYMERix demonstrated, it did not sell well and lacked acceptance and was thus removed from market just 4 years after its initial release, leaving the public with no options for immunization against Lyme disease.⁵¹ 20 years later, the target that GSK utilized for their vaccine formulation, outer surface protein A (OspA), has been resurrected by the Austrian pharmaceutical company Valneva.⁵² In partnership with Pfizer, their alum-adjuvanted OspA-based recombinant protein vaccine VLA15 has successfully undergone phase II clin-

Here, we demonstrated that OspA mRNA-LNP displayed superior immunogenicity and efficacy to an alum-adjuvanted OspA protein subunit vaccine when used at doses of 3 μg and 1 μg , respectively. First, mice immunized with a single dose of OspA mRNA-LNP elicited more robust polyfunctional CD8⁺ and CD4⁺ T cell responses than the OspA protein vaccine. Though antibody response is the key to preventing *B. burgdorferi* infection in the host, anti-OspA CD8⁺ T cells could provide further immune support as spirochetes in some patients express OspA in late infection.⁶⁴ Second, one particular subset of CD4⁺ T cells, Tfh cells, along with antigen-specific GC B cells, were more greatly elevated in mice after a single vaccination with OspA mRNA-LNP than in mice immunized with rOspA + alum. Increased magnitude of germinal center responses corresponded to increased levels of its terminal outputs, antigen-specific MBCs and LLPCs, which secreted IgG1, IgG2a, and IgG2b, after immunization with a single dose of OspA mRNA-LNP. Third, a prime-boost regimen of OspA mRNA-LNP compared to one of rOspA + alum yielded higher, longer-lasting levels of OspA-specific antibodies, which are crucial to blocking transmission of *B. burgdorferi* to the host from feeding ticks.⁶⁵ Most importantly, a single dose of OspA mRNA-LNP more successfully protected mice from *B. burgdorferi* infection than its recombinant protein comparator. Recombinant OspA has been previously shown to be fully protective in mice when administered at much higher doses and with multiple boosters, but this study utilizes a single low-dose regimen that offers partial protection.⁶⁶ Finally, although mice were challenged by needle injection in this study, an OspA mRNA-LNP vaccine could be highly effective against tick challenge, which represents the natural route of infection.

Despite the prevalence of Lyme disease, there is no commercially available FDA-approved vaccine for humans. Here, we show that a novel nucleoside-modified OspA mRNA-LNP vaccine could provide prophylactic protection against *B. burgdorferi* infection. The immunogenicity and protective efficacy of OspA mRNA-LNP outperformed alum-adjuvanted recombinant OspA protein, which is analogous to the highly effective LYMERix vaccine released by GSK in 1998. While mainly used against viruses, these studies further illustrate that the mRNA-LNP vaccine platform can be applied to bacterial targets as well. With further preclinical and clinical development, OspA mRNA-LNP could prove to be a viable preventative approach to curtailing the pervasiveness of Lyme disease.

MATERIALS AND METHODS

Ethics statement

The investigators faithfully adhered to the “Guide for the Care and Use of Laboratory Animals” by the Committee on Care of Laboratory Animal Resources Commission on Life Sciences, National Research Council. Mouse studies were conducted under protocols approved by the Institutional Animal Care and Use Committees (IACUC) of the University of Pennsylvania (UPenn). All animals were housed and cared for according to local, state, and federal policies in an Association for Assessment and Accreditation of Laboratory Animal Care International (AAALAC)-accredited facility.

Bacteria, protein, and cells

Lipidated OspA protein⁶⁷ and *Borrelia burgdorferi* (strain N40) from the laboratories of Dustin Brisson at the University of Pennsylvania and Erol Fikrig at Yale University, respectively, were used for vaccination and challenge studies. *Bb* N40 was cultured in BSK-H Medium, Complete (Sigma-Aldrich, St. Louis, MO) at 33°C in a Shake ‘N’ Bake Hybridization Oven (Boekel Scientific, Feasterville-Treose, PA). Neuro-2a cells (CCL-131, ATCC, Manassas, VA) were cultured in DMEM + GlutaMAX (Gibco, Waltham, MA), 10% heat-inactivated (HI) FBS (Gemini Bio, West Sacramento, CA), and 100 units/mL penicillin and 100 $\mu\text{g}/\text{mL}$ streptomycin (Gibco) at 37°C and 5% CO₂.

mRNA production

Codon-optimized OspA (from *B. burgdorferi* strain B31)- and firefly luciferase (Luc)-gene-containing plasmids were synthesized (GenScript, Piscataway, NJ). Plasmids were then linearized, and a T7-driven *in vitro* transcription reaction (Life Technologies, Carlsbad, CA) was performed to generate mRNA with 101 nucleotide long poly(A) tails. The 5' UTR utilizes the tobacco etch virus leader sequence, and the 3' UTR contains sequences from the human beta-globin gene. Capping of mRNA was performed in concert with transcription through addition of a trinucleotide cap1 analog CleanCap, and m1 Ψ -5'-triphosphate (TriLink, San Diego, CA) was incorporated into the reaction instead of uridine-5'-triphosphate (UTP). Cellulose-based purification of mRNA was performed as described.⁶⁸ mRNAs were then checked on an agarose gel before storing at -20°C.

Lipid nanoparticle formulation of mRNA

Purified mRNAs were encapsulated in lipid nanoparticles using a self-assembling ethanolic lipid mixture of an ionizable cationic lipid, 1,2-distearoyl-*sn*-glycero-3-phosphocholine, cholesterol, and a polyethylene glycol-lipid as previously described.⁶⁹ This mixture was rapidly combined with an aqueous solution containing mRNA at acidic pH. The ionizable cationic lipid (pKa in the range of 6.0–6.5), proprietary to Acuitas Therapeutics (Vancouver, Canada), and LNP composition are described in the patent application WO 2017/004143. The average hydrodynamic diameter was ~80 nm with a polydispersity index of 0.02–0.06 as measured by dynamic light scattering using a Zetasizer Nano ZS (Malvern Instruments, Malvern, UK) and an encapsulation efficiency of ~95% as determined using a Quant-iT Ribogreen assay (Life Technologies).

mRNA transfection

Transfection of Neuro-2a cells was performed utilizing TransIT-mRNA (Mirus Bio, Madison, WI), according to the manufacturer's instructions: mRNA (0.1 μg) was combined with TransIT-mRNA Reagent and Boost Reagent in 17 μL serum-free medium, and the complex was added to 3×10^4 cells in 183 μL complete medium.

Western blot analysis

After overnight incubation at 37°C, mRNA-transfected cells were lysed for 30 min on ice in radio immunoprecipitation assay buffer (Sigma-Aldrich). Whole-cell lysate from mRNA-transfected cells

was assayed for OspA protein by denaturing SDS-PAGE western blot. 5 μ L of cell lysate (obtained from 1.5×10^4 cells) was diluted in 4X Laemmli buffer (Bio-Rad, Hercules, CA) containing β -mercaptoethanol and incubated at 95°C for 5 min and then separated on a 4%–15% precast polyacrylamide Mini-Protean TGX gel (Bio-Rad) for 1 h at 120 V. Transfer to polyvinylidene fluoride membrane was completed utilizing an iBlot 2 Dry Blotting System (Thermo Fisher, Waltham, MA). The membrane was blocked with 5% non-fat dry milk in Tris-buffered saline (TBS) buffer containing 0.1% Tween 20 (Sigma-Aldrich). OspA protein was probed by incubating with a 1:1,000 dilution of rabbit polyclonal OspA antibody (Rockland Immunochemicals, Pottstown, PA) overnight at 4°C, followed by incubation with a 1:5,000 dilution of goat anti-rabbit horseradish peroxidase (HRP)-IgG (ImmunoResearch Laboratories, West Grove, PA) secondary antibody for 1 h at room temperature, where both antibodies were diluted in 5% non-fat dry milk in TBS-T. Blots were washed three times for 15 min each with TBS-T before and after addition of secondary antibody and developed using Amersham ECL Western Blotting Detection Reagent (Cytiva, Marlborough, MA) on an Amersham Imager 600 (GE Healthcare, Chicago, IL). After detection of OspA protein, membranes were stripped with Restore Stripping Buffer (Thermo Fisher), washed, blocked, and re-probed by incubating with a 1:500 dilution of anti-beta tubulin antibody (Abcam, Cambridge, UK) overnight at 4°C, followed by incubation with donkey anti-rabbit secondary antibody as before. Blots were washed and developed as previously described.

Mouse immunizations

Female Balb/c mice, 8 weeks of age, were purchased from Charles River Laboratories (Wilmington, MA). Mice were immunized intramuscularly with a 50 μ L volume of 3 μ g mRNA-LNP encoding either OspA or Luc in PBS or 1 μ g rOspA + alum in saline for both prime and booster doses. Aluminum hydroxide (Alhydrogel adjuvant 2%, InvivoGen, San Diego, CA) was adsorbed to recombinant protein by incubating for 2 h at room temperature.

Flow cytometry analysis of innate cells in mouse muscle at injection site

Muscle tissue was obtained from the injection site (right gastrocnemius) of each immunized mouse and minced using forceps and scissors. Each sample was digested in a total volume of 10 mL XMedia (Ham's F12 Nutrient Mix [Gibco], 10% FBS [Gemini Bio], and 100 units/mL penicillin and 100 μ g/mL streptomycin [Gibco]) containing 100 units/mL collagenase, type IV (Gibco) and 1.1 units/mL dispase II (Roche, Basel, Switzerland) for 30 min at 37°C while shaking. Supernatant was filtered through a 70- μ m cell strainer and washed in PBS. After digestion, filtering (of remaining post-digest suspension), and PBS washes were repeated, each sample was resuspended in 1 mL XMedia. 3×10^6 cells per sample were washed with PBS and stained with a LIVE/DEAD Fixable Aqua Dead Cell Stain Kit (Life Technologies) for 10 min in the dark at room temperature (RT). Cells were subsequently incubated for 30 min at 4°C with a cocktail containing the following fluorescently labeled anti-mouse monoclonal antibodies: CD11c, CD45, I-A/I-E (MHC-II), CD24, CD11b, Ly-6G,

CD64, and F4/80. Antibodies used in these studies can be found in Table S1. The panel was derived from Yu et al.⁷⁰ Cells were washed with fluorescence-activated cell sorting (FACS) buffer (PBS with 2% HI FBS) and then fixed with 1% paraformaldehyde (PFA) for 30 min prior to acquisition. All samples were acquired on a modified LSR II flow cytometer (BD Biosciences). 500,000 events were collected per specimen, and data were analyzed with FlowJo v10 software (Treestar, Woodburn, OR).

Flow cytometry analysis of polyfunctional T cells in mouse splenocytes

Single-cell suspensions of mouse splenocytes were generated in complete RPMI-1640 medium. 3×10^6 cells per sample were stimulated for 6 h at 37°C and 5% CO₂ in the presence of a pool of 66 overlapping 15-mer OspA peptides (GenScript) at 1.5 μ g/mL and anti-CD28 antibody (clone 37.51, BD Biosciences, Franklin Lakes, NJ) at 1 μ g/mL. GolgiPlug (Brefeldin A, BD Biosciences) at 5 μ g/mL and GolgiStop (Monensin, BD Biosciences) at 10 μ g/mL were added to each sample 1 h after the start of stimulation. Unstimulated samples for each animal were also included. A sample stimulated with phorbol 12-myristate-13-acetate (Sigma-Aldrich) at 10 μ g/mL and ionomycin (Sigma-Aldrich) at 200 ng/mL was included as a positive control. After stimulation, cells were washed with PBS and stained with a LIVE/DEAD Fixable Aqua Dead Cell Stain Kit (Life Technologies) for 10 min in the dark at RT. Cells were subsequently surface stained with unlabeled CD16/CD32 rat anti-mouse (clone 2.4G2, BD Biosciences) and anti-CD4 PerCP (peridinin chlorophyll protein)/Cy5.5 (clone GK1.5, BioLegend, San Diego, CA) and anti-CD8 Pacific Blue (clone 53-6.7, BioLegend) monoclonal antibodies (mAbs) for 30 min in the dark at 4°C. After surface staining, cells were washed with FACS buffer, fixed (PBS containing 1% PFA), and permeabilized using a Permeabilization/Fixation Solution Kit (with GolgiPlug or GolgiStop, BD Biosciences). Cells were then intracellularly stained with anti-CD3 allophycocyanin (APC)-Cy7 (clone 145-2C11, BD Biosciences), anti-tumor necrosis factor (TNF)- α phycoerythrin (PE)-Cy7 (clone MP6-XT22, BD Biosciences), anti-interferon (IFN)- γ Alexa Fluor 700 (AF700) (clone XMG1.2, BD Biosciences), and anti-interleukin (IL)-2 Brilliant Violet 711 (BV711) (clone JES6-5H4, BioLegend) monoclonal antibodies for 30 min in the dark at 4°C. Finally, cells were washed with permeabilization buffer, fixed as before, and stored at 4°C until analysis. Splenocytes were analyzed on a modified LSR II flow cytometer (BD Biosciences). 500,000 events were collected per specimen. After the gates for each function were developed, the Boolean gate platform was used to create the full array of possible combinations, equating to seven response patterns when testing three functions. Data were analyzed with FlowJo v10 software (Treestar). Data were expressed by subtracting frequencies of unstimulated stained cells from frequencies of peptide pool-stimulated stained samples.

Preparation of fluorescent OspA B cell tetramers for flow cytometry

Recombinant OspA protein (Prospec, Rehovot, HaMerkaz, Israel) was biotinylated using the EZ-Link MicroSulfo-NHS-Biotinylation

Kit (Thermo Fisher). Streptavidin-conjugated Alexa Fluor 488 and 647 (Thermo Fisher) were then individually added at a 6:1 M ratio (biotinylated protein to streptavidin-conjugate) to separate vials of biotinylated protein. The total volume of each fluorochrome was split into 10 subaliquots, and these subaliquots were then added, on ice, to the biotinylated protein and mixed by pipetting every 10 min (for a total of 10 additions).

Flow cytometry analysis of GC B/Tfh cells in mouse splenocytes and lymph nodes

Spleen and draining lymph nodes (inguinal and popliteal) were harvested 12 days post immunization, homogenized with a syringe plunger, and filtered through a 40- μ m cell strainer on ice. Splenocytes were then subjected to red blood cell lysis for 7 min in 2 mL ACK buffer on ice and resuspended in 2 mL DMEM (with 10% HI FBS). All staining steps were carried out at 4°C in FACS buffer (PBS with 2% HI FBS and 5 mM EDTA). Single-cell suspensions were Fc blocked with anti-CD16/CD32 (clone 2.4G2, BioXCell, Lebanon, NH) monoclonal antibody prior to staining.

Tfh cell staining

Cells were incubated with biotinylated CXCR5 for 1 h and then washed. Cells were incubated for 30 min with a cocktail of Fixable Viability dye eFluor780, streptavidin BV421, and the following fluorescently labeled anti-mouse monoclonal antibodies: B220, CD4, CD44, CD62L, and PD-1. Antibodies used in these studies can be found in Table S2. Cells were washed with FACS buffer and then fixed and permeabilized in FoxP3/Transcription Factor Staining Buffer Set (eBioScience, San Diego, CA) according to manufacturer's instructions before intranuclear staining with BCL6 for 30 min. All incubations were performed at 4°C.

GC B cell staining

Cells were incubated with biotinylated CD138 for 1 h and then washed. Cells were incubated for 30 min at 4°C with a cocktail containing Fixable Viability dye eFluor780, streptavidin BV650, OspA AF488 tetramer, OspA AF647 tetramer, RBD BV421 tetramer, and the following cocktail of fluorescently labeled anti-mouse monoclonal antibodies: CD19, FAS, GL7, IgD, and CD3. Antibodies used in these studies can be found in Table S3. Excess antibodies were washed away, and cells were fixed with 1% PFA for 30 min prior to acquisition. All samples were acquired on a fiber laser Aurora (Cytek, Fremont, CA), and data were analyzed in FlowJo v10.

Flow cytometry analysis of MBCs/LLPCs in mouse splenocytes and bone marrow

Splenocytes were harvested from spleens by mechanical disruption between frosted slides and filtered through 63- μ m Nitex mesh. Bone marrow was flushed from femurs and tibia from each mouse using a 23G X $\frac{3}{4}$ " needle and syringe into FACS buffer and filtered through 63- μ m Nitex mesh. Splenocytes and bone marrow cells were then subjected to RBC lysis for 5 min in ACT buffer on ice. 5 million cells were then stained with fixable live dead aqua (Zombie Aqua, BioLegend, 1:500 in PBS) for 15 min at RT. Cells

were then washed with FACS buffer and stained with the respective dilutions of antibodies in Table S4 in BD Brilliant Staining Buffer (BD Biosciences) for 15 min at 4°C. 2.5 million events per sample were acquired on a BD Symphony A3 Lite and analyzed with FlowJo v10 software.

ELISpot assay

Bone marrow was flushed from femurs and tibia from each mouse using a 23G X $\frac{3}{4}$ " needle and syringe into FACS buffer and filtered through 63- μ m Nitex mesh. Red blood cells were lysed in ACT buffer for 5 min on ice. Resulting cells were counted using a Beckman Coulter (Brea, CA) ViCell. MultiScreenHTS IP Filter Plate, 0.45 μ m (Millipore Sigma, Burlington, MA), was coated with recombinant OspA protein (Prospec) at 5 μ g/mL in sodium carbonate/sodium bicarbonate buffer (pH 9.6) (35 mM NaHCO₃ and 15 mM Na₂CO₃) for 1 h at 37°C. Plates were then washed with 200 μ L PBS/well three times and blocked at 37°C in complete RPMI + 10% FBS for 30 min. Bone marrow (BM) cells were plated in six halving dilutions beginning with 1 million total BM cells per well and incubated overnight in complete RPMI + 10% FBS. Plates were then washed with wash buffer (1x PBS + 0.1% Tween 20) five times and incubated with various biotinylated anti-IgG detection antibodies (Table S5) in PBS + 2% BSA at RT for 1 h. Plates were once again washed five times, and streptavidin-alkaline phosphatase (1:20,000 dilution in PBS + 2% BSA) was added prior to incubation at RT for 30 min. Plates were then washed five times with wash buffer, and 50 μ L/well BCIP/NBT single solution (Sigma-Aldrich) was added for ~ 5 min or until spots developed, at which time the reaction was quenched with 100 μ L 1 M sodium phosphate monobasic solution. After plates were rinsed with dH₂O and dried overnight, they were scanned and counted using CTL (Shaker Heights, OH) Immunospot hardware and software.

Enzyme-linked immunosorbent assay

Determination of OspA-specific IgG titers

96-well EIA/RIA Clear Flat Bottom Polystyrene High Bind Microplates (Corning) were coated with recombinant OspA protein (Prospec) in PBS at a final concentration of 0.1 μ g per well and allowed to incubate overnight at 4°C. Plates were then washed three times with 0.05% Tween 20 (Sigma-Aldrich) in PBS (PBS-T) and blocked in 2% BSA (Sigma-Aldrich) in PBS (blocking buffer) for 1 h at RT. After washing three times as before, serum samples were 3-fold serially diluted in blocking buffer and allowed to incubate at RT for 2 h. Plates were then washed three times again with PBS-T, and HRP-conjugated anti-mouse secondary antibody (Jackson ImmunoResearch Laboratories) was added at a concentration of 1:10,000 in blocking buffer and incubated at RT for 1 h. Plates were washed one final time as before and developed using KPL 2-component TMB Microwell Peroxidase Substrate (Seracare, Milford, MA) for 6 min before quenching with 2N sulfuric acid (Sigma-Aldrich). Absorbance was measured at 450 nm using a SpectraMax (Molecular Devices, San Jose, CA) 190 microplate reader. OspA-specific IgG endpoint dilution titer was defined as the highest dilution of serum to give an optical

density (OD) greater than the sum of the background OD plus 0.01 units. All samples were run in technical duplicates.

Quantification of *Borrelia burgdorferi* burden

C₆ peptide ELISA was performed according to previously published methods.^{71–73} 96-well EIA/RIA Clear Flat Bottom Polystyrene High Bind Microplates (Corning) were coated with C₆ peptide⁷¹ (GenScript) in 100 mM aqueous sodium carbonate (Sigma-Aldrich) at a final concentration of 1 µg per well and allowed to incubate overnight at 4°C. Plates were then washed three times with 0.05% Tween 20 (Sigma-Aldrich) in PBS (PBS-T) and blocked in 5% BSA (Sigma-Aldrich) in PBS (blocking buffer) for 1 h at RT. After washing three times as before, serum samples were diluted 1:900 in diluent buffer (1% BSA) and allowed to incubate at RT for 1 h. Plates were then washed three times again with PBS-T, and HRP-conjugated anti-mouse secondary antibody (Jackson ImmunoResearch Laboratories) was added at a concentration of 1:10,000 in diluent buffer and incubated at RT for 1 h. Plates were washed one final time as before and developed using KPL 2-component TMB Microwell Peroxidase Substrate (Seracare) for 10 min before quenching with 2N sulfuric acid (Sigma-Aldrich). Absorbance was measured at 450 nm using a SpectraMax (Molecular Devices) 190 microplate reader.

In vivo infection of mice

Mice were immunized with 3 µg OspA mRNA-LNP or Luc mRNA-LNP or 1 µg rOspA + alum. 4 weeks after immunization, mice were injected subcutaneously with 1×10^5 *Borrelia burgdorferi* N40. 25 days post infection, mice were sacrificed, and bladder, heart, joint (knee), and skin (ear) samples were harvested for qPCR. For long-term challenge studies, mice were given an equivalent booster immunization at 4 weeks, injected subcutaneously 35 weeks post prime with 1×10^5 *Borrelia burgdorferi* N40, and sacrificed 25 days later. Spleens were harvested for tissue culture.

Quantification of *Borrelia burgdorferi* burden by qPCR

One-half of each bladder, heart, joint, and skin tissue (split bilaterally with scissors) was lysed, and DNA was extracted using a DNeasy Blood and Tissue Kit (Qiagen, Hilden, Germany). Quantitative polymerase chain reaction (qPCR) was performed with Itaq Universal SYBR (Bio-Rad) and DNA using *flagellin* (*flaB*), a *Borrelia*-specific marker gene, and mouse β -*actin* specific primers for normalization. Samples were run in technical triplicates on a QuantStudio 3 Real-Time PCR System (Applied Biosystems, Waltham, MA). *B. burgdorferi* load values are equal to the average of $2^{(Ct[\beta\text{-actin}] - Ct[\textit{flaB}])}$ of all technical replicates for each sample. Primer nucleotide sequences can be found in Table S6.

Quantification of *Borrelia burgdorferi* burden by tissue culture

One-third of each spleen was added to a 1.5-µL parafilm-sealed Eppendorf tube filled with BSK-H Medium, Complete (Sigma-Aldrich) and amphotericin-B (2.5 µg/mL; Sigma-Aldrich), rifampicin (50 µg/mL; Sigma-Aldrich), and phosphomycin (20 µg/mL; Sigma-Aldrich) and incubated at 33°C in an Imperial III incubator (Lab Line Instruments, Melrose Park, IL). After 5 days, cultures were as-

sessed by dark-field microscopy (Axiostar Plus, Zeiss, Oberkochen, Germany) for the presence of motile spirochetes.

Statistical analyses

Statistical analyses were performed using Prism 9 (GraphPad Software, San Diego, CA). Data were compared, and differences were considered statistically significant by one-way ANOVA with Bonferroni correction (*p < 0.05, **p < 0.01, ***p < 0.001, ****p < 0.0001).

DATA AND CODE AVAILABILITY

All data are available within the article and its supplemental information file or from the authors upon request.

SUPPLEMENTAL INFORMATION

Supplemental information can be found online at <https://doi.org/10.1016/j.ymthe.2023.07.022>.

ACKNOWLEDGMENTS

We thank Ben Davis and Mohamad-Gabriel Alameh (University of Pennsylvania) for the discussions about qPCR and flow cytometry. We thank Majed Ghattas (Polytechnique Montréal) for the muscle digestion protocol. We thank Tristan Nowak (University of Albany, NYSDoH) for his expertise in *Borrelia burgdorferi* detection methods. The graphical abstract, and Figures 1A, 4A, 5A, and S6A were created with BioRender. N.P. and E.F. were supported by the National Institute of Allergy and Infectious Diseases (N.P., R01AI146101 and R01AI153064; E.F., AI126033, AI165499 and AI138949) D.W. received funding from BioNTech RNA Pharmaceuticals. E.F. and D.W. receive support from the Steven and Alexandra Cohen Foundation and the Howard Hughes Medical Institute Emerging Pathogens Program. D.B. receives support from Burroughs Wellcome Fund BWF1012376 and NIAID R01AI142572 and R21AI137433. M.L. was supported by NIH NIAID grants R01AI153064 and R01AI168312.

AUTHOR CONTRIBUTIONS

N.P. and M.P. conceived the study. N.P., M.P., D.W., G.A., T.M.H., E.B., B.T.G., E.F., and I.T. designed and performed experiments. N.P., D.W., M.P., G.A., T.M.H., E.B., B.T.G., I.T., M.L., D.A., D.B., T.K., and E.F. reviewed and interpreted data. H.M. and Y.K.T. contributed to vaccine production. M.P. drafted and all authors contributed to manuscript preparation. All authors had access to data and gave final approval before submission.

DECLARATION OF INTERESTS

In accordance with the University of Pennsylvania policies and procedures and our ethical obligations as researchers, we report that D.W. is named on patents that describe the use of nucleoside-modified mRNA as a platform to deliver therapeutic proteins. N.P., D.W., and Y.K.T. are named on a patent describing the use of nucleoside-modified mRNA in lipid nanoparticles as a vaccine platform. We have disclosed those interests fully to the University of Pennsylvania, and we have in place an approved plan for managing any potential conflicts arising from licensing of our patents. Y.K.T. is an employee

of Acuitas Therapeutics, a company focused on the development of LNP nucleic acid delivery systems for therapeutic applications. N.P. served on the mRNA strategic advisory board of Sanofi Pasteur in 2022. N.P. is a member of the scientific advisory board of AldexChem.

REFERENCES

- Mead, P.S. (2015). Epidemiology of Lyme disease. *Infect. Dis. Clin. North Am.* 29, 187–210.
- Kugeler, K.J., Farley, G.M., Forrester, J.D., and Mead, P.S. (2015). Geographic Distribution and Expansion of Human Lyme Disease, United States. *Emerg. Infect. Dis.* 21, 1455–1457.
- Kugeler, K.J., Schwartz, A.M., Delorey, M.J., Mead, P.S., and Hinckley, A.F. (2021). Estimating the Frequency of Lyme Disease Diagnoses, United States, 2010–2018. *Emerg. Infect. Dis.* 27, 616–619.
- Nadelman, R.B. (2015). Erythema Migrans. *Infect. Dis. Clin. North Am.* 29, 211–239.
- Aucott, J.N., and Seifert, A. (2011). Misdiagnosis of early Lyme disease as the summer flu. *Orthop. Rev.* 3, e14.
- Donta, S.T. (2012). Issues in the diagnosis and treatment of Lyme disease. *Open Neurol. J.* 6, 140–145.
- Murray, T.S., and Shapiro, E.D. (2010). Lyme Disease. *Clin. Lab. Med.* 30, 311–328.
- Nadelman, R.B., Hanincová, K., Mukherjee, P., Liveris, D., Nowakowski, J., McKenna, D., Brisson, D., Cooper, D., Bittker, S., Madison, G., et al. (2012). Differentiation of Reinfection from Relapse in Recurrent Lyme Disease. *N. Engl. J. Med.* 367, 1883–1890.
- Coleman, J.L., Roemer, E.J., and Benach, J.L. (1999). Plasmin-coated borrelia burgdorferi degrades soluble and insoluble components of the mammalian extracellular matrix. *Infect. Immun.* 67, 3929–3936.
- Lagal, V., Portnoi, D., Faure, G., Postic, D., and Baranton, G. (2006). Borrelia burgdorferi sensu stricto invasiveness is correlated with OspC-plasminogen affinity. *Microbes Infect.* 8, 645–652.
- Önder, Ö., Humphrey, P.T., McOmber, B., Korobova, F., Francella, N., Greenbaum, D.C., and Brisson, D. (2012). OspC is potent plasminogen receptor on surface of Borrelia burgdorferi. *J. Biol. Chem.* 287, 16860–16868.
- Radolf, J.D., Caimano, M.J., Stevenson, B., and Hu, L.T. (2012). Of ticks, mice and men: understanding the dual-host lifestyle of Lyme disease spirochaetes. *Nat. Rev. Microbiol.* 10, 87–99.
- Steere, A.C., Strle, F., Wormser, G.P., Hu, L.T., Branda, J.A., Hovius, J.W.R., Li, X., and Mead, P.S. (2016). Lyme borreliosis. *Nat. Rev. Dis. Primers* 2, 16090.
- Tracy, K.E., and Baumgarth, N. (2017). *Borrelia burgdorferi* Manipulates Innate and Adaptive Immunity to Establish Persistence in Rodent Reservoir Hosts. *Front. Immunol.* 8, 116.
- Schwan, T.G., Piesman, J., Golde, W.T., Dolan, M.C., and Rosa, P.A. (1995). Induction of an outer surface protein on Borrelia burgdorferi during tick feeding. *Proc. Natl. Acad. Sci. USA* 92, 2909–2913.
- Kenedy, M.R., Lenhart, T.R., and Akins, D.R. (2012). The role of *Borrelia burgdorferi* outer surface proteins. *FEMS Immunol. Med. Microbiol.* 66, 1–19.
- Khatchikian, C.E., Nadelman, R.B., Nowakowski, J., Schwartz, I., Levy, M.Z., Brisson, D., and Wormser, G.P. (2015). Public health impact of strain specific immunity to *Borrelia burgdorferi*. *BMC Infect. Dis.* 15, 472.
- Fikrig, E., Barthold, S.W., Kantor, F.S., and Flavell, R.A. (1990). Protection of mice against the Lyme disease agent by immunizing with recombinant OspA. *Science (New York, N.Y.)* 250, 553–556.
- Steere, A.C., Sikand, V.K., Meurice, F., Parenti, D.L., Fikrig, E., Schoen, R.T., Nowakowski, J., Schmid, C.H., Laukamp, S., Buscarino, C., and Krause, D.S. (1998). Vaccination against Lyme disease with recombinant Borrelia burgdorferi outer-surface lipoprotein A with adjuvant. Lyme Disease Vaccine Study Group. *N. Engl. J. Med.* 339, 209–215.
- Gross, D.M., Forsthuber, T., Tary-Lehmann, M., Etling, C., Ito, K., Nagy, Z.A., Field, J.A., Steere, A.C., and Huber, B.T. (1998). Identification of LFA-1 as a Candidate Autoantigen in Treatment-Resistant Lyme Arthritis. *Science (New York, N.Y.)* 281, 703–706.
- Steere, A.C., Drouin, E.E., and Glickstein, L.J. (2011). Relationship between immunity to Borrelia burgdorferi outer-surface protein A (OspA) and Lyme arthritis. *Clin. Infect. Dis.* 52, s259–s265.
- Nigrovic, L.E., and Thompson, K.M. (2007). The Lyme vaccine: a cautionary tale. *Epidemiol. Infect.* 135, 1–8.
- Gomes-Solecki, M. (2014). Blocking pathogen transmission at the source: reservoir targeted OspA-based vaccines against Borrelia burgdorferi. *Front. Cell. Infect. Microbiol.* 4, 136.
- Grosenbaugh, D.A., De Luca, K., Durand, P.Y., Feilmeier, B., DeWitt, K., Sigoillot-Claude, C., Sajous, M.L., Day, M.J., and David, F. (2018). Characterization of recombinant OspA in two different Borrelia vaccines with respect to immunological response and its relationship to functional parameters. *BMC Vet. Res.* 14, 312.
- Camire, A.C., Hatke, A.L., King, V.L., Millership, J., Ritter, D.M., Sobell, N., Weber, A., and Marconi, R.T. (2021). Comparative analysis of antibody responses to outer surface protein (Osp)A and OspC in dogs vaccinated with Lyme disease vaccines. *Vet. J.* 273, 105676.
- Nayak, A., Schüller, W., Seidel, S., Gomez, I., Meinke, A., Comstedt, P., and Lundberg, U. (2020). Broadly Protective Multivalent OspA Vaccine against Lyme Borreliosis, Developed Based on Surface Shaping of the C-Terminal Fragment. *Infect. Immun.* 88, e00917–e00919.
- Gomes-Solecki, M., Arnaboldi, P.M., Backenson, P.B., Benach, J.L., Cooper, C.L., Dattwyler, R.J., Diuk-Wasser, M., Fikrig, E., Hovius, J.W., Laegreid, W., et al. (2019). Protective Immunity and New Vaccines for Lyme Disease. *Clin. Infect. Dis.* 70, 1768–1773.
- Pardi, N., Hogan, M.J., Pelc, R.S., Muramatsu, H., Andersen, H., DeMaso, C.R., Dowd, K.A., Sutherland, L.L., Searce, R.M., Parks, R., et al. (2017). Zika virus protection by a single low-dose nucleoside-modified mRNA vaccination. *Nature* 543, 248–251.
- Pardi, N., Parkhouse, K., Kirkpatrick, E., McMahon, M., Zost, S.J., Mui, B.L., Tam, Y.K., Karikó, K., Barbosa, C.J., Madden, T.D., et al. (2018). Nucleoside-modified mRNA immunization elicits influenza virus hemagglutinin stalk-specific antibodies. *Nat. Commun.* 9, 3361.
- Pardi, N., Carreño, J.M., O'Dell, G., Tan, J., Bajusz, C., Muramatsu, H., Rijnink, W., Strohmeier, S., Loganathan, M., Bielak, D., et al. (2022). Development of a pentavalent broadly protective nucleoside-modified mRNA vaccine against influenza B viruses. *Nat. Commun.* 13, 4677.
- McMahon, M., O'Dell, G., Tan, J., Sárközy, A., Vadovics, M., Carreño, J.M., Puente-Massaguer, E., Muramatsu, H., Bajusz, C., Rijnink, W., et al. (2022). Assessment of a quadrivalent nucleoside-modified mRNA vaccine that protects against group 2 influenza viruses. *Proc. Natl. Acad. Sci. USA* 119, e2206333119.
- Alameh, M.G., Weissman, D., and Pardi, N. (2022). Messenger RNA-Based Vaccines Against Infectious Diseases. *Curr. Top. Microbiol. Immunol.* 440, 111–145.
- Pardi, N., Hogan, M.J., Porter, F.W., and Weissman, D. (2018). mRNA vaccines — a new era in vaccinology. *Nat. Rev. Drug Discov.* 17, 261–279.
- Hogan, M.J., and Pardi, N. (2022). mRNA Vaccines in the COVID-19 Pandemic and Beyond. *Annu. Rev. Med.* 73, 17–39.
- Corbett, K.S., Edwards, D., Leist, S.R., Abiona, O.M., Boyoglu-Barnum, S., Gillespie, R.A., Himansu, S., Schäfer, A., Ziwawo, C.T., DiPiazza, A.T., et al. (2020). SARS-CoV-2 mRNA vaccine design enabled by prototype pathogen preparedness. *Nature* 586, 567–571.
- Polack, F.P., Thomas, S.J., Kitchin, N., Absalon, J., Gurtman, A., Lockhart, S., Perez, J.L., Pérez Marc, G., Moreira, E.D., Zerbini, C., et al. (2020). Safety and Efficacy of the BNT162b2 mRNA Covid-19 Vaccine. *N. Engl. J. Med.* 383, 2603–2615.
- D'Souza, W.N., and Lefrançois, L. (2004). Frontline: An in-depth evaluation of the production of IL-2 by antigen-specific CD8 T cells in vivo. *Eur. J. Immunol.* 34, 2977–2985.
- Pardi, N., Hogan, M.J., Naradikian, M.S., Parkhouse, K., Cain, D.W., Jones, L., Moody, M.A., Verkerke, H.P., Myles, A., Willis, E., et al. (2018). Nucleoside-modified mRNA vaccines induce potent T follicular helper and germinal center B cell responses. *J. Exp. Med.* 215, 1571–1588.

39. Lederer, K., Castaño, D., Gómez Atria, D., Oguin, T.H., 3rd, Wang, S., Manzoni, T.B., Muramatsu, H., Hogan, M.J., Amanat, F., Cherubin, P., et al. (2020). SARS-CoV-2 mRNA Vaccines Foster Potent Antigen-Specific Germinal Center Responses Associated with Neutralizing Antibody Generation. *Immunity* 53, 1281–1295.e5.
40. Alameh, M.G., Tombácz, I., Bettini, E., Lederer, K., Sittplangkoon, C., Wilmore, J.R., Gaudette, B.T., Soliman, O.Y., Pine, M., Hicks, P., et al. (2021). Lipid nanoparticles enhance the efficacy of mRNA and protein subunit vaccines by inducing robust T follicular helper cell and humoral responses. *Immunity* 54, 2877–2892.e7.
41. Lederer, K., Bettini, E., Parvathaneni, K., Painter, M.M., Agarwal, D., Lundgreen, K.A., Weirick, M., Muralidharan, K., Castaño, D., Goel, R.R., et al. (2022). Germinal center responses to SARS-CoV-2 mRNA vaccines in healthy and immunocompromised individuals. *Cell* 185, 1008–1024.e15.
42. Bettini, E., Lederer, K., Sharpe, H., Kaminski, M., Jones, L., and Locci, M. (2022). A combined fine needle aspiration and spectral flow cytometry approach to assess human germinal center responses to SARS-CoV-2 vaccination. *STAR Protoc.* 3, 101840.
43. Sallusto, F., Lanzavecchia, A., Araki, K., and Ahmed, R. (2010). From vaccines to memory and back. *Immunity* 33, 451–463.
44. Laczko, D., Hogan, M.J., Toulmin, S.A., Hicks, P., Lederer, K., Gaudette, B.T., Castaño, D., Amanat, F., Muramatsu, H., Oguin, T.H., 3rd, et al. (2020). A Single Immunization with Nucleoside-Modified mRNA Vaccines Elicits Strong Cellular and Humoral Immune Responses against SARS-CoV-2 in Mice. *Immunity* 53, 724–732.
45. Gupta, A., Arora, G., Rosen, C.E., Kloos, Z., Cao, Y., Cerny, J., Sajid, A., Hoornstra, D., Golovchenko, M., Rudenko, N., et al. (2020). A human secretome library screen reveals a role for Peptidoglycan Recognition Protein 1 in Lyme borreliosis. *Plos Pathog.* 16, e1009030.
46. Stone, B.L., Tourand, Y., and Brissette, C.A. (2017). Brave New Worlds: The Expanding Universe of Lyme Disease. *Vector Borne Zoonotic Dis.* 17, 619–629.
47. Bobe, J.R., Jutras, B.L., Horn, E.J., Embers, M.E., Bailey, A., Moritz, R.L., Zhang, Y., Soloski, M.J., Ostfeld, R.S., Marconi, R.T., et al. (2021). Recent Progress in Lyme Disease and Remaining Challenges. *Front. Med.* 8, 666554.
48. Steere, A.C., Malawista, S.E., Snyderman, D.R., Shope, R.E., Andiman, W.A., Ross, M.R., and Steele, F.M. (1977). An epidemic of oligoarticular arthritis in children and adults in three connecticut communities. *Arthritis Rheum.* 20, 7–17.
49. Steere, A.C. (2020). Posttreatment Lyme disease syndromes: distinct pathogenesis caused by maladaptive host responses. *J. Clin. Invest.* 130, 2148–2151.
50. Rebman, A.W., and Aucutt, J.N. (2020). Post-treatment Lyme Disease as a Model for Persistent Symptoms in Lyme Disease. *Front. Med.* 7, 57.
51. Plotkin, S.A. (2011). Correcting a public health fiasco: The need for a new vaccine against Lyme disease. *Clin. Infect. Dis.* 52, s271–s275.
52. Comstedt, P., Schüler, W., Meinke, A., and Lundberg, U. (2017). The novel Lyme borreliosis vaccine VLA15 shows broad protection against *Borrelia* species expressing six different OspA serotypes. *PLoS One* 12, e0184357.
53. Dattwyler, R.J., and Gomes-Solecki, M. (2022). The year that shaped the outcome of the OspA vaccine for human Lyme disease. *NPJ Vaccin.* 7, 10.
54. Comstedt, P., Hanner, M., Schüler, W., Meinke, A., and Lundberg, U. (2014). Design and development of a novel vaccine for protection against Lyme borreliosis. *PLoS One* 9, e113294.
55. Pardi, N., Hogan, M.J., and Weissman, D. (2020). Recent advances in mRNA vaccine technology. *Curr. Opin. Immunol.* 65, 14–20.
56. Awasthi, S., Hook, L.M., Pardi, N., Wang, F., Myles, A., Cancro, M.P., Cohen, G.H., Weissman, D., and Friedman, H.M. (2019). Nucleoside-modified mRNA encoding HSV-2 glycoproteins C, D, and E prevents clinical and subclinical genital herpes. *Sci. Immunol.* 4, eaaw7083.
57. Mallory, K.L., Taylor, J.A., Zou, X., Waghela, I.N., Schneider, C.G., Sibilo, M.Q., Punde, N.M., Perazzo, L.C., Savransky, T., Sedegah, M., et al. (2021). Messenger RNA expressing PfCSP induces functional, protective immune responses against malaria in mice. *NPJ Vaccin.* 6, 84.
58. Hayashi, C.T.H., Cao, Y., Clark, L.C., Tripathi, A.K., Zavala, F., Dwivedi, G., Knox, J., Alameh, M.G., Lin, P.J.C., Tam, Y.K., et al. (2022). mRNA-LNP expressing PfCSP and Pfs25 vaccine candidates targeting infection and transmission of *Plasmodium falciparum*. *NPJ Vaccin.* 7, 155.
59. Sajid, A., Matias, J., Arora, G., Kurokawa, C., DePonte, K., Tang, X., Lynn, G., Wu, M.J., Pal, U., Strank, N.O., et al. (2021). mRNA vaccination induces tick resistance and prevents transmission of the Lyme disease agent. *Sci. Transl. Med.* 13, eabj9827.
60. Matias, J., Kurokawa, C., Sajid, A., Narasimhan, S., Arora, G., Diktas, H., Lynn, G.E., DePonte, K., Pardi, N., Valenzuela, J.G., et al. (2021). Tick immunity using mRNA, DNA and protein-based Salp14 delivery strategies. *Vaccine* 39, 7661–7668.
61. Kon, E., Levy, Y., Elia, U., Cohen, H., Hazan-Halevy, I., Aftalion, M., Ezra, A., Bar-Haim, E., Naidu, G.S., Diesendruck, Y., et al. (2023). A single-dose F1-based mRNA-LNP vaccine provides protection against the lethal plague bacterium. *Sci Adv* 9, eadg1036.
62. Osterloh, A. (2022). Vaccination against Bacterial Infections: Challenges, Progress, and New Approaches with a Focus on Intracellular Bacteria. *Vaccines (Basel)* 10, 751.
63. Price, V.L., and Kieny, M.P. (2001). Vaccines for parasitic diseases. *Curr. Drug Targets Infect. Disord.* 1, 315–324.
64. Anguita, J., Hedrick, M.N., and Fikrig, E. (2003). Adaptation of *Borrelia burgdorferi* in the tick and the mammalian host. *FEMS Microbiol. Rev.* 27, 493–504.
65. de Silva, A.M., Telford, S.R., 3rd, Brunet, L.R., Barthold, S.W., and Fikrig, E. (1996). *Borrelia burgdorferi* OspA is an arthropod-specific transmission-blocking Lyme disease vaccine. *J. Exp. Med.* 183, 271–275.
66. Fikrig, E., Barthold, S.W., Kantor, F.S., and Flavell, R.A. (1992). Long-term protection of mice from Lyme disease by vaccination with OspA. *Infect. Immun.* 60, 773–777.
67. Voordouw, M.J., Tupper, H., Önder, Ö., Devevey, G., Graves, C.J., Kemps, B.D., and Brisson, D. (2013). Reductions in human Lyme disease risk due to the effects of oral vaccination on tick-to-mouse and mouse-to-tick transmission. *Vector Borne Zoonotic Dis.* 13, 203–214.
68. Baiersdorfer, M., Boros, G., Muramatsu, H., Mahiny, A., Vlatkovic, I., Sahin, U., and Karikó, K. (2019). A Facile Method for the Removal of dsRNA Contaminant from In Vitro-Transcribed mRNA. *Mol. Ther. Nucleic Acids* 15, 26–35.
69. Pardi, N., Tuyishime, S., Muramatsu, H., Kariko, K., Mui, B.L., Tam, Y.K., Madden, T.D., Hope, M.J., and Weissman, D. (2015). Expression kinetics of nucleoside-modified mRNA delivered in lipid nanoparticles to mice by various routes. *J. Control Release* 217, 345–351.
70. Yu, Y.R.A., O’Koren, E.G., Hotten, D.F., Kan, M.J., Kopin, D., Nelson, E.R., Que, L., and Gunn, M.D. (2016). A Protocol for the Comprehensive Flow Cytometric Analysis of Immune Cells in Normal and Inflamed Murine Non-Lymphoid Tissues. *PLoS One* 11, e0150606.
71. Chen, Y.L., Marcinkiewicz, A.L., Nowak, T.A., Tyagi Kundu, R., Liu, Z., Strych, U., Bottazzi, M.E., Chen, W.H., and Lin, Y.P. (2022). CspZ FH-Binding Sites as Epitopes Promote Antibody-Mediated Lyme Borreliae Clearance. *Infect. Immun.* 90, e0006222.
72. Nowak, T.A., Lown, L.A., Marcinkiewicz, A.L., Sürth, V., Kraiczky, P., Burke, R., and Lin, Y.P. (2023). Outer surface protein E (OspE) mediates *Borrelia burgdorferi* sensu stricto strain-specific complement evasion in the eastern fence lizard, *Sceloporus undulatus*. *Ticks Tick. Borne. Dis.* 14, 102081.
73. Liang, F.T., Bowers, L.C., and Philipp, M.T. (2001). C-terminal invariable domain of VlsE is immunodominant but its antigenicity is scarcely conserved among strains of Lyme disease spirochetes. *Infect. Immun.* 69, 3224–3231.

YMTHE, Volume 31

Supplemental information

Development of an mRNA-lipid nanoparticle vaccine against Lyme disease

Matthew Pine, Gunjan Arora, Thomas M. Hart, Emily Bettini, Brian T. Gaudette, Hiromi Muramatsu, István Tombácz, Taku Kambayashi, Ying K. Tam, Dustin Brisson, David Allman, Michela Locci, Drew Weissman, Erol Fikrig, and Norbert Pardi

Supplemental Information

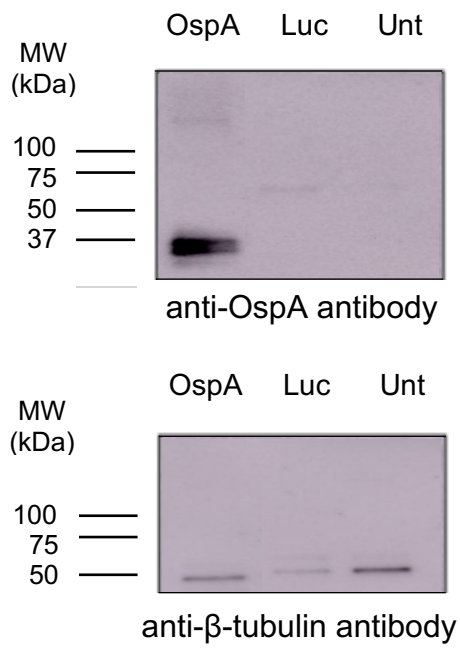


Figure S1. Protein production from OspA mRNA *in vitro*. Neuro 2-a cells were transfected with OspA- or Luc-encoding mRNAs. OspA protein expression in whole-cell lysate was detected by Western blot, utilizing untransfected cells (Unt) and Luc mRNA-transfected cells as negative controls. Membrane was stripped and re-probed with anti-beta tubulin antibody as a loading control. MW: molecular weight

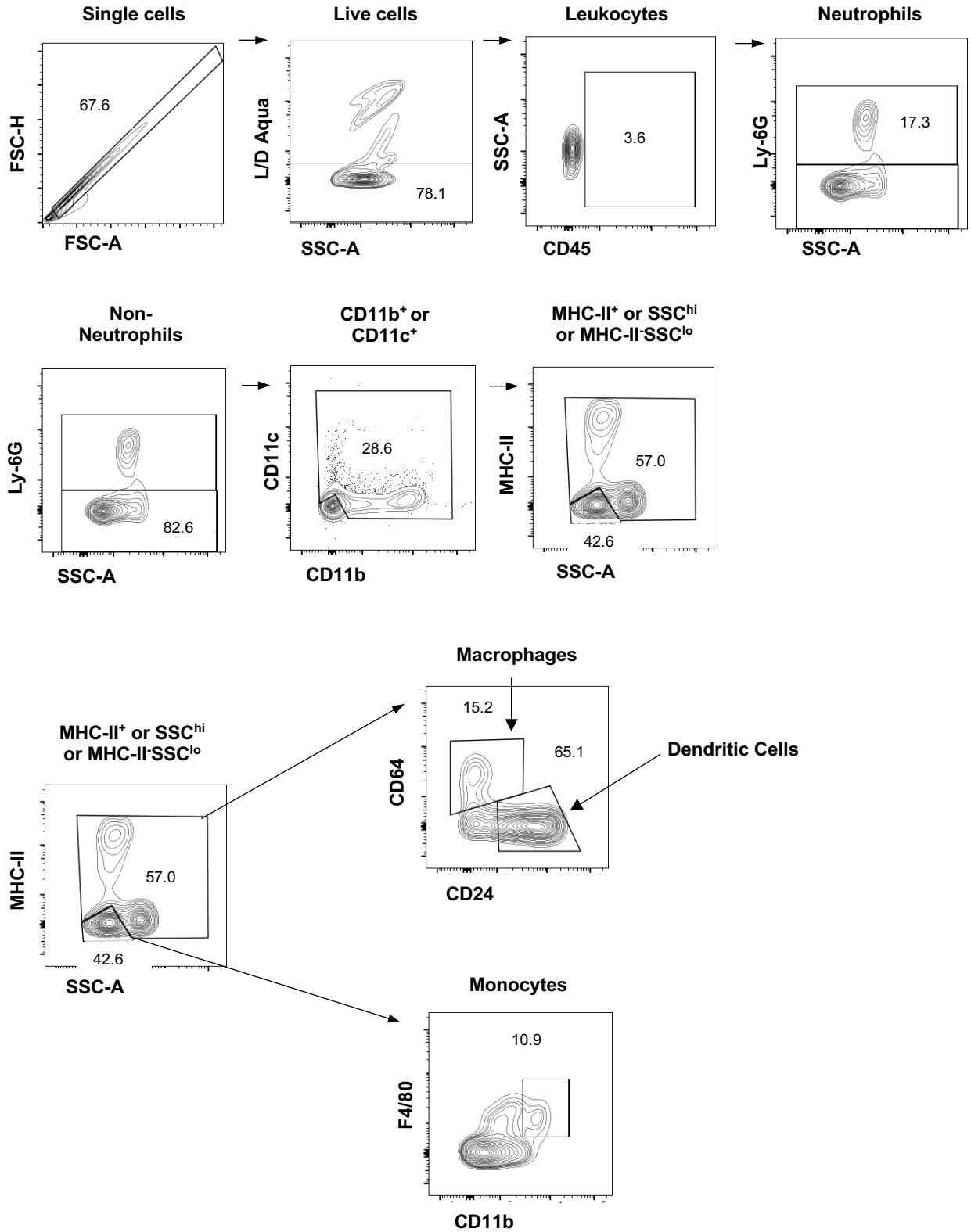


Figure S2. Flow cytometric gating strategy for the investigation of innate immune cell responses after *OspA* mRNA-LNP and r*OspA* + alum immunizations in mice. Representative flow cytometry plots for innate immune cell populations (neutrophils, macrophages, dendritic cells, monocytes).

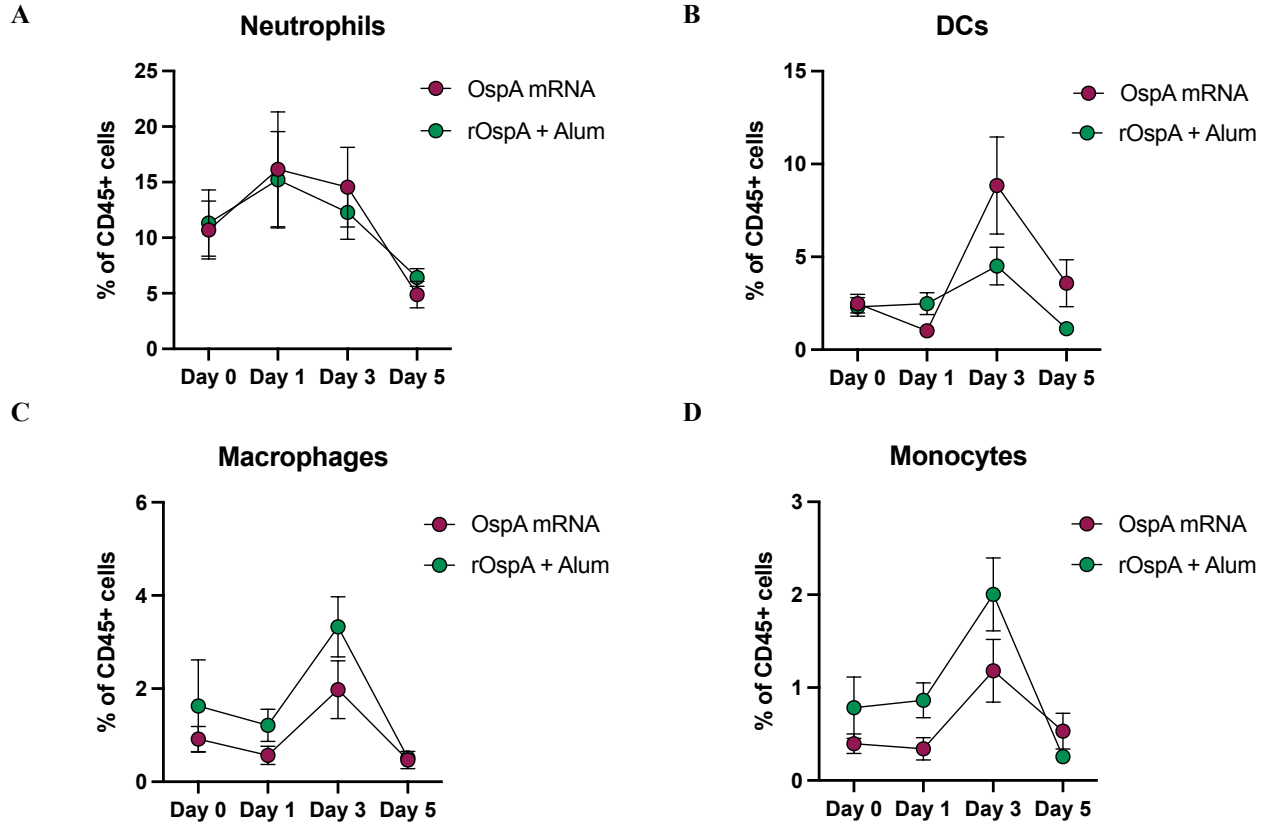


Figure S3. Assessing innate cell populations in injection site muscle of immunized mice. Mice were vaccinated intramuscularly with a single dose of 3 μ g of OspA mRNA-LNP or 1 μ g of rOspA + alum and innate immune cell responses were assessed 1, 3 and 5 days post injections. Non-injected mice were used as controls (day 0). Frequencies of (A) neutrophils ($CD45^+Ly-6G^+$) (B) dendritic cells ($CD45^+Ly-6G^-CD11b/CD11c^+MHCII^+/SSC^{hi}CD64^+CD24^+$) (C) macrophages ($CD45^+Ly-6G^-CD11b/CD11c^+MHCII^+/SSC^{hi}CD64^+CD24^+$) and (D) monocytes ($CD45^+Ly-6G^-CD11b/CD11c^+MHCII^+/SSC^{lo}CD11b^{hi}F4/80^+$) Data represent mean \pm SEM (n = 5 mice per group). Data from one experiment is shown.

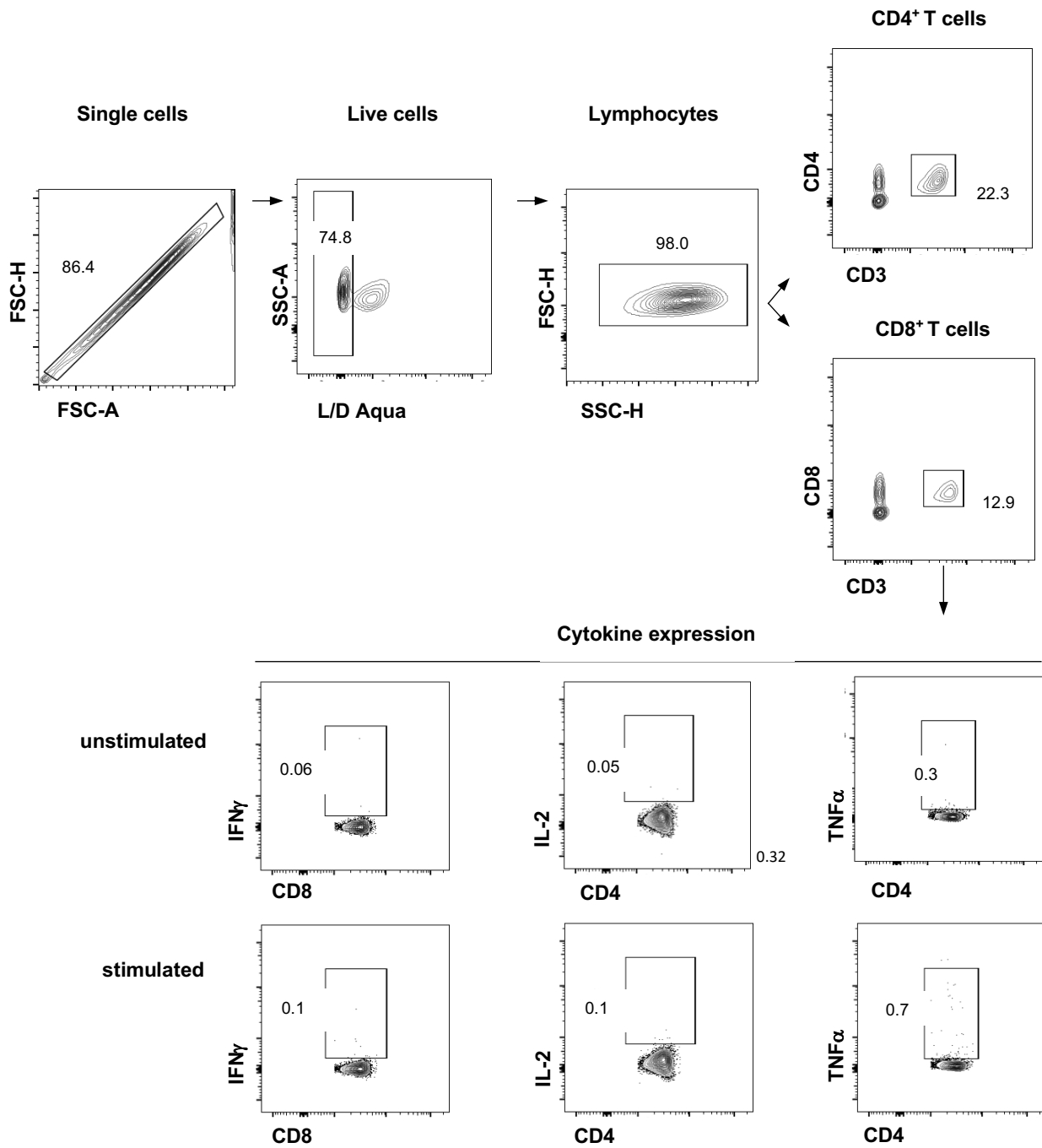
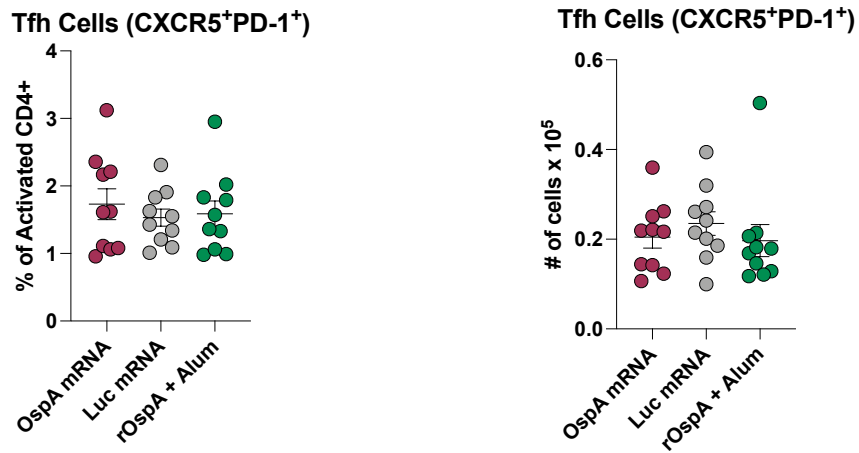


Figure S4. Flow cytometric gating strategy for the investigation of T cell responses in Ospa mRNA-LNP-immunized mice. Representative flow cytometry plots for unstimulated and peptide-stimulated samples are shown.

A



B

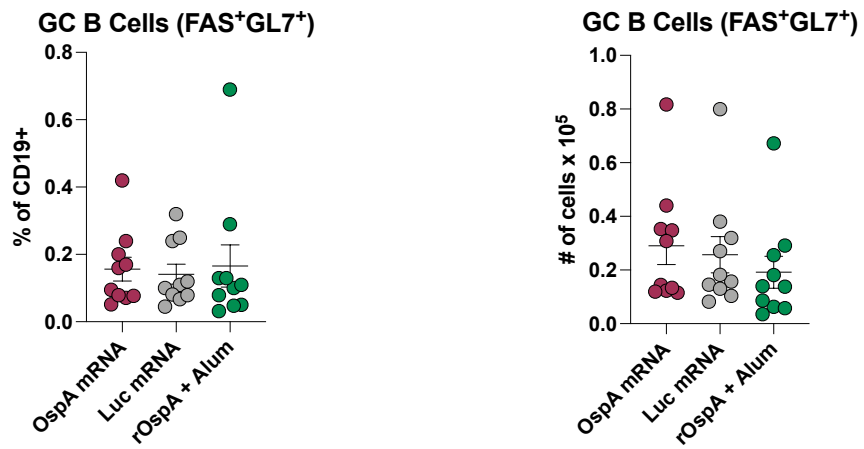
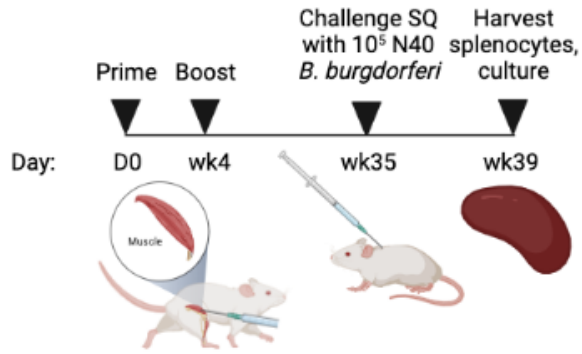


Figure S5. Assessing T follicular helper and germinal center B cells in spleens of immunized mice. (A) Tfh cell (B220⁻CD4⁺CD62L⁻PD-1⁺CXCR5⁺) frequencies (left panel) and absolute numbers (right panel). (B) GC B cell (CD19⁺CD3⁺FAS⁺GL7⁺) frequencies (left panel) and absolute numbers (right panel). Each symbol represents one animal, and data represent mean ± SEM (n = 10 mice per group). Data from two independent experiments are shown.

A**B**

Vaccine	Culture
OspA mRNA-LNP	0/5
Luc mRNA-LNP	4/4
rOspA + alum	0/5

Figure S6. Nucleoside-Modified OspA mRNA-LNP immunization protects mice from infection with *Borrelia burgdorferi* (A) Mice were vaccinated and boosted intramuscularly with OspA or Luc mRNA-LNPs or rOspA + alum as described in Figure 4. Thirty-five weeks after the prime dose, mice were challenged subcutaneously with 10^5 *Borrelia burgdorferi* (strain N40) and then sacrificed 25 days later. Splenocytes were cultured for detection of *B. burgdorferi* infection. (B) Number of animals with detectable *B. burgdorferi* burden five days after spleen harvest. Data is obtained from one experiment.

Table S1. Antibodies used for innate cell flow cytometry

Stain	Fluorochrome	Clone	Vendor	Catalog #
CD11c	BV421	N418	BioLegend	117330
CD45	BV605	30-F11	BioLegend	103139
I-A/I-E	BV650	M5/114.15.2	BD Biosciences	563415
CD24	BV711	M1/69	BD Biosciences	563405
CD11b	APC-Cy7	M1/70	BD Biosciences	557657
Ly-6G	AF700	1A8	BD Biosciences	561236
CD64	PE-CF594	X54-5/7.1	BioLegend	139320
F4/80	PE	BM8	BioLegend	123109

Table S2. Antibodies used for T follicular helper (Tfh) cell flow cytometry.

Stain	Fluorochrome	Clone	Vendor	Catalog #
CXCR5	Biotin	SPRCL5	eBioscience	13-7185-82
Streptavidin	BV421	-	BioLegend	405225
B220	BV650	RA3-6B2	BioLegend	103241
CD4	PerCP-Cy5.5	RM4-5	BioLegend	100540
CD44	BV605	IM7	BioLegend	103047
CD62L	BUV395	MEL-14	BD	740218
PD-1	PE	RMP1-30	BioLegend	109104
Bcl6	AF647	K112-91	BD	624024
Live/Dead	eFluor 780	-	eBioscience	65-0865-14

Table S3. Antibodies used for germinal center B (GC B) cell flow cytometry.

Stain	Fluorochrome	Clone	Vendor	Catalog #
CD138	Biotin	281-2	BD Biosciences	553713
Streptavidin	BV650	-	BioLegend	405232
CD3e	BUV395	145-2c11	BD Biosciences	563565
CD19	BV605	6D5	BioLegend	115540
GL7	PerCP-Cy5.5	GL7	BioLegend	144610
FAS	PE	Jo2	BD Biosciences	554258
IgD	PE-Cy7	11-26c.2a	BioLegend	405720
OspA Tetramer 1	AF488	-	Labeled in-house	See methods
OspA Tetramer 2	AF647	-	Labeled in-house	See methods
RBD Tetramer	BV421	-	Labeled in-house	See methods
Live/Dead	eFluor 780	-	eBioscience	65-0865-14

Table S4. Antibodies used for memory B cell (MBC) and long-lived plasma (LLPC) cell flow cytometry.

Stain	Fluorochrome	Clone	Vendor	Catalog #
B220	BV421	RA3-6B2	BioLegend	103240
CD138	BB700	281-2	BD Biosciences	742124
CD38	AF700	90	Invitrogen	56-0381-82
IgD	APC-Cy7	11-26C.2A	BioLegend	405716
CD19	BV711	6D5	BioLegend	115555
GL7	PE	GL7	BioLegend	144608
FAS	PE-Cy7	Jo2	BD Biosciences	55763
CD4	PE-Cy5	H129.19	BD Biosciences	553654
CD8a	PE-Cy5	53-6.7	BD Biosciences	553034
Ter-119	PE-Cy5	TER119	BioLegend	116210
F4/80	PE-Cy5	BM8	Invitrogen	15-4801-82
OspA Tetramer 1	AF488	-	Labeled in-house	See methods
OspA Tetramer 2	AF657	-	Labeled in-house	See methods

Table S5. Antibodies used for long-lived plasma cell (LLPC) ELISpot assays.

Stain	Conjugate	Clone	Vendor	Catalog #
IgG1	biotin	polyclonal	Southern Biotech	1070-08
IgG2a	biotin	polyclonal	Southern Biotech	1080-08
IgG2b	biotin	polyclonal	Southern Biotech	1090-08
IgG3	biotin	polyclonal	Southern Biotech	1100-08
ExtrAvidin	alkaline phosphatase	-	Sigma-Aldrich	E2636

Table S6. Primers used for *Borrelia burgdorferi* detection.

Primer	Sequence
<i>mactin</i> F	CATTGCTGACAGGATGCAGAAGG
<i>mactin</i> R	TGCTGGAAGCTGGACAGTGAGG
<i>flaB</i> F	ACAGCTGAAGAGCTTGAATG
<i>flaB</i> R	CTTGTTTGCTCCAACATGAAC